

1018

**GEOCHEMISTRY OF THE AMPHIBOLITIC  
HOST ROCKS OF THE HUTTI GOLD FIELDS,  
KARNATAKA**

**DISSERTATION SUBMITTED TO THE  
JAWAHARLAL NEHRU UNIVERSITY  
in partial fulfilment of the requirements for the  
award of the degree of  
MASTER OF PHILOSOPHY**

78P + fig + tables

**T.S. GIRITHARAN**

**SCHOOL OF ENVIRONMENTAL SCIENCES  
JAWAHARLAL NEHRU UNIVERSITY  
NEW DELHI**

**JUNE 1993**



जवाहरलाल नेहरु विश्वविद्यालय  
JAWAHARLAL NEHRU UNIVERSITY  
NEW DELHI - 110067

## CERTIFICATE

This dissertation entitled "Geochemistry of amphibolitic host rocks of the Hutti Gold Fields, Karnataka", embodies the work carried out at the School of Environmental Sciences, J.N.U., New Delhi. This work has not been submitted in part or in full, for any degree or diploma of any university.

*T.S. Giritharan*  
[ T.S. GIRITHARAN ]

*V. Subramanian* 29/6/93  
PROF. V. SUBRAMANIAN  
(Dean)

*V. Rajamani* 25/6/93  
PROF. V. RAJAMANI  
( Supervisor )

SCHOOL OF ENVIRONMENTAL SCIENCES  
JAWAHARLAL NEHRU UNIVERSITY  
NEW DELHI.

## ACKNOWLEDGEMENT

With great pleasure, I express my deep sense of gratitude to Prof. V. RAJAMANI, for the guidance and encouragement rendered to me during the course of this work.

I gratefully acknowledge Prof. Gilbert N. Hanson and Dr. James Sevigney of the State University of New York at Stonybrook, for the discussions I had with them during my field work. I thank Mr. Karadi, Mr. Raju, and Mr. Naresh Kumar of Hutti Gold Mines Ltd., and Mr. Prabhakar Sangurmath of M.E.C.L. for the Logistic support during my field work.

My sincere thanks goes to Dean, S.E.S., J.N.U., for Providing necessary research facilities to carry out the present work smoothly.

Financial assistance in the form of J.R.F. from J.N.U. and U.G.C. are gratefully acknowledged.

I am thankful to my senior friends Dr. Siddaiah, Dr. Balakrishnan and Dr. Zachariah for the discussions I had with them. It is a great pleasure to express my thanks to my colleagues Mr. Manoj Mohanta, Mr. Jayant Tripathi, Mr. Anupam Sharma and the Lab. attendant Mr. Krishnamurthy for their cooperation during the Laboratory works. Mr. Jayaram Sahu, Mr. Asokan and Mr. Amar Singh of Roorkee University helped me during my stay at Roorkee for some analytical work.

Mr. Saini and Mr. Bhupender Upadhyay helped me with their secretarial skills.

Last but not the least, I thank everybody who helped me in completing this work and whose name has not been mentioned here.

DATE : 25-6-93

PLACE : NEW DELHI.

  
(T.S. GIRITHARAN)

# CONTENTS

Page No.

CHAPTER-I - INTRODUCTION .....	1
1.1 : Crustal evolution, metallogeny and its importance. ....	1
1.2 : Dharwar Craton of South India .....	2
1.3 : Gold mineralization in the schist belts of the eastern Dharwar craton .....	7
CHAPTER-II - HUTTI - THE AREA OF STUDY .....	12
2.1 : Location and accessibility .....	12
2.2 : Physiography and Climate .....	12
2.3 : Previous Work .....	14
2.4 : Geology of the Hutti-Maski schist belt .....	16
2.5 : Field observations .....	22
2.6 : Petrography .....	26
CHAPTER-III - ANALYTICAL PROCEDURES .....	35
3.1 : Sample Processing .....	35
3.2 : Sample Dissolution .....	36
3.2.1 : Preparation of "B" - solution .....	36
3.2.2 : Gravimetric determination of silica by Alkali fusion .....	37
3.2.3 : Preparation of Sample Solution by $\text{LiBO}_2$ -Fusion .....	38
3.3 : Analysis of major and trace elements by ICP-AES .....	40
3.3.1 : The Instrument .....	40
3.3.2 : Preparation of Standard solutions and instrument calibration ..	40
3.3.3 : Precision and Accuracy .....	41
CHAPTER-IV - GEOCHEMICAL RESULTS AND DISCUSSION .....	43
CHAPTER-V - CONCLUSION .....	62
REFERENCES .....	64

## LIST OF TABLES

Page No.

Table 1.1	:	Generalised chronology for the Karnataka Nucleus .....	6
Table 3.1	:	Analytical Wavelengths, Nature and concentrations of solutions used for analyses. All analyses by ICP-AES except Na and K by Flame Photometer. ....	39
Table 3.2	:	Accuracy of major and trace element data of IRS (analysed by ICP-AES) used for calibration of the instrument. ....	42
Table 4.1	:	Major and trace element data of the Hutti meta tholeiites. ....	44
Table 4.1.(a):		Symbols used in the text and table 4.1. ....	46
Table 4.2	:	Calculated cation mole percentages of Hutti meta tholeiites. ....	48
Table 4.3	:	Normative mineral composition (in percentage) of mafic rocks from Hutti schist belt. ....	50
Table 4.4	:	Plotting parameters for the CA-M-S Projection diagram for the Hutti Meta tholeiites. ....	61

## LIST OF FIGURES

PAGE NO.

Fig. 1.1	: Geological map of South India Showing Dharwar craton, granulite terrane and Younger Covers. HSB denotes Hutti schist Belt, RSB- Ramagiri schist belt and KSB- Kolar schist belt. ....	3
Fig. 2.1	: Location map of Hutti, Karnataka. ....	13
Fig. 2.2	: Geological map of Hutti-Maski Schist Belt ....	17
Fig. 2.3	: Generalised structural map of the Hutti-Maski schist belt. ....	19
Fig. 2.4	: Structural features of the Hutti-Maski schist belt. ....	20

## FIELD PHOTOGRAPHS

Plate1-Fig.2.5	: Amphibolites in tectonic contact with the granite. ....	72
Plate1-Fig.2.6	: Intrusive contact of mafic rocks with the granite ....	72
Plate2-Fig.2.7	: F3 type open fold in the amphibolite ....	73
Plate2-Fig.2.8	: Pyroclastics in the Pamankallur area ....	73
Plate3-Fig.2.9	: Undeformed clastic pebbles in the conglomerate horizon of Palkanmardi area ....	74
Plate3-Fig.2.10	: Deformed clastic pebbles in the conglomerate of Palkanmardi area ....	74

## PHOTOMICROGRAPHS

**PAGE NO.**

Plate4-Fig.2.11:	Hornblende Augen in sample # GH-4 .....	75
Plate4-Fig.2.12:	Deformed actinolite crystal in GH-4 .....	75
Plate5-Fig.2.13:	Schistose amphibolite-sample GH-7 .....	76
Plate5-Fig.2.14:	Fibrous aggregates of actinolite in sample # GH-14 .....	76
Plate6-Fig.2.15:	Trident shaped calcite vein in chlorite schist .....	77
Plate6-Fig.2.16:	Calcite vein cutting the schistosity in chlorite schist .....	77
Plate7-Fig.2.17:	Opagues in the coarse grained amphibolite .....	78
Plate7-Fig.2.18:	Relict igneous texture in sample GH-17 .....	78
Fig.4.1 :	Jenson's diagram for the classification of Hutti meta tholeiites .....	47
Fig.4.2 :	Cation mole percent Mgo Vs FeO diagram (Hanson and Langmuir, 1978) .....	51
Fig.4.3 :	[Mg] versus [Fe] plot for Hutti meta tholeiites .....	52
Fig.4.4 :	Comparison of Hutti metatholeiites with Kolar and Ramagiri tholeiites in the [Mg] versus [Fe] plot. ....	55
Fig.4.5 :	Ni versus Zr plot for the Hutti tholeiites .....	57
Fig.4.6 :	[Fe] Versus Zr plot .....	58
Fig.4.7 :	CA-M-S Projection diagram for the Hutti meta tholeiites .....	60

# CHAPTER 1

## INTRODUCTION

### 1.1. CRUSTAL EVOLUTION, METALLOGENY AND ITS IMPORTANCE

The Earth was formed through the accretion of planetesimals. Heat energy released as a result of accretion melted the earth which began to differentiate into core, mantle and crust. Large scale Earth differentiation processes have played a significant role in the development and evolution of the crust, and the materials which constitute the crust.

An understanding of the Earth's internal processes is essential in studies involving crustal genesis and the mineralization associated with it. Earth's internal processes can be studied with the help of commonly occurring mantle derived magmatic rocks and rarely occurring mantle derived peridotite nodules. It is these internal processes of the earth which initiates and drives the external processes such as the well documented Phanerozoic style plate tectonic processes. Understanding of such processes have an important bearing on the evolution of the crust and the formation of mineral deposits associated with them. The present study is aimed at unravelling the geodynamic processes responsible for the continental crust formation and evolution in the gold mineralized Hutti schist belt of the eastern Dharwar craton. This area is chosen because, in addition to understanding the crustal



evolution, this study will be of economic importance, in terms of understanding the processes responsible for gold mineralization, since gold mineralization, is thought to be associated with accretionary tectonic regimes resulting from subduction processes. (Rajamani, 1991). Thus it becomes an essential requisite for any resource management programme.

## **1.2. DHARWAR CRATON OF SOUTH INDIA**

The cratonic block of south India covers an area of 2,38,000 km<sup>2</sup> lying between latitudes 12° O' and 18° O' and longitudes 74° O' and 80° O' forming the heart of peninsular India. This block originally formed a part of the Gondwana land atleast until the end of paleozoic and its truncated extensions to the west and east are to be traced in Africa and Antarctica respectively. Though the bulk of the crust making the Dharwar craton formed prior to 2,500 M.Y., ago, an Early Proterozoic Mobile Belt (EPMB) event remobilised the crust through the processes of sedimentation, Amphibolite grade metamorphism (in the northern part) granulite grade metamorphism, (in the southern part) and Co<sub>2</sub> -K Metasomatism, thus producing the Southern high grade province and a northern granite-greenstone province.

The northern block is further divided into an eastern gold field province, and a western iron-manganese ore province with reference to k-rich granites (closepet granite) in the central part. The north eastern margin of the Dharwar

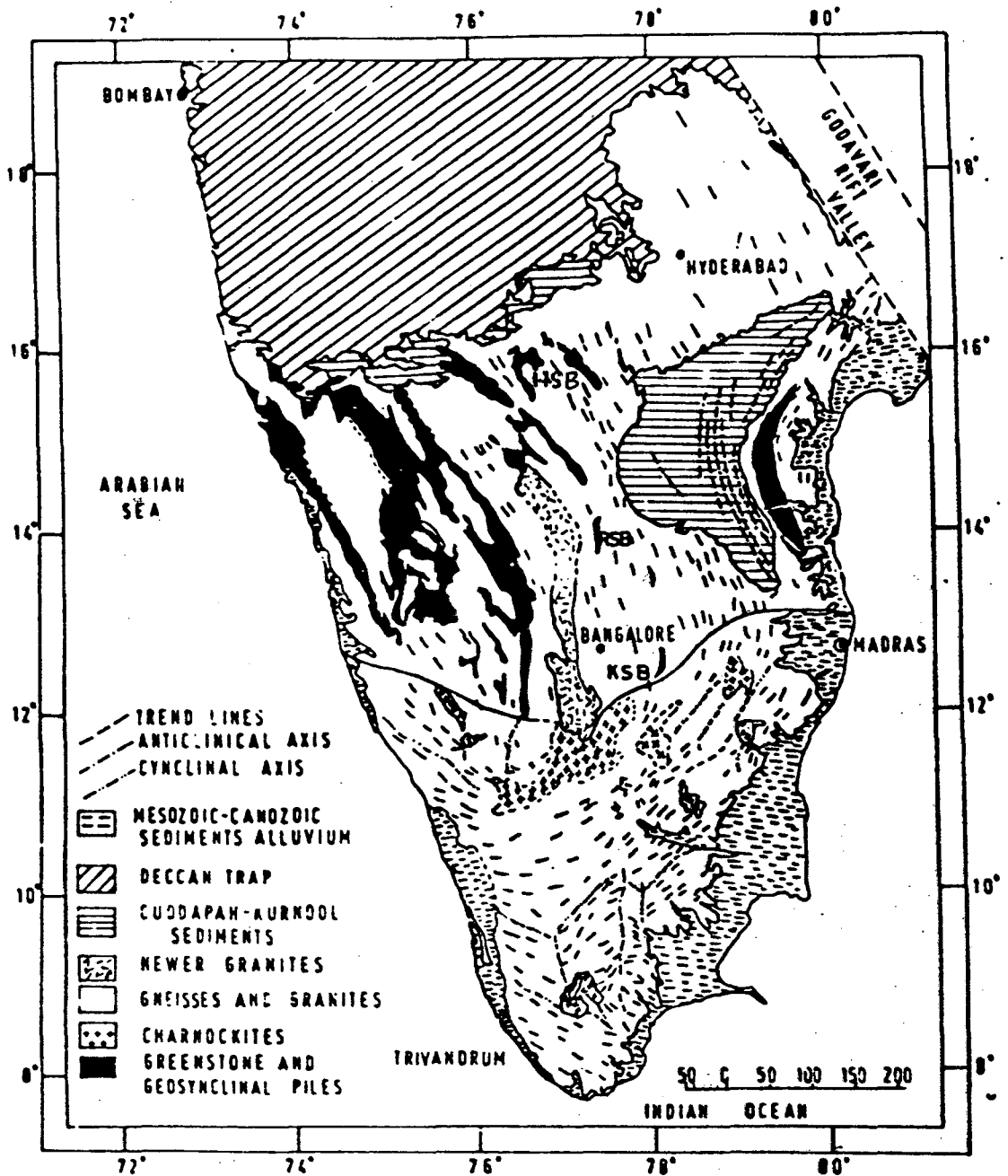


Fig. 1.1 Geological map of South India, showing Dharwar craton, granulite terrane and younger covers. HSB denotes Hutti Schist Belt, RSB denotes Ramagiri Schist Belt, and KSB, Kolar Schist Belt.

craton is limited by the Godavari graben, a structural element active since the Proterozoic. Gold occurs sporadically in the schist belts of the eastern Dharwar craton and is believed to be remobilised during the EPMB event. (Radhakrishna and Naqvi, 1986). The limits of various provinces and the location of the gold mineralised schist belts are shown in the fig. 1.1.

Since the south Indian shield forms a coherent crustal segment in which the geological activity can be traced continuously throughout the precambrian, it is a classic area for the study of different stages of the early crustal evolution, (Radhakrishna, 1986). The current thinking prevalent on the various stages of crustal evolution in the Karnataka craton can be summarised as follows :

The elliptical shaped cratonic nuclei commonly referred as the Karnataka Nuclei (KN) was formed prior to 3400 M.Y. There is no clearcut evidence to say how this cratonic nuclei was formed. This nuclei is made up of rocks generally older than 2,500 M.Y. and mainly composed of low grade schist-gneiss sequences. A major controversy is centered around the schist- (greenstone)-gneiss relationship. Three views are prevalent as to the schist - gneiss relationship.

(1) The Dharwar schist (greenstone) belts represent a group of rocks younger than the hybrid Peninsular Gneisses and there exists an older sargur group which predates the gneisses. ( Swaminath and Ramakrishnan, 1981).

(2) Together the Dharwar supra crustals and the sargurs represent one "supergroup" older than the peninsular gneisses. (Pichamuthu and srinivasan, 1984).  
and

(3) The Archaean Supra crustals represent belts formed at different periods covering a span of atleast 1000 M.Y. (3500-2500M.Y.), some of which are older and some younger than the gneisses which are themselves polyphase and polymetamorphic ( Naqvi, 1981; Radhakrishna, 1983; Naqvi and Rogers, 1983).

The Early Proterozoic Mobile Belt (EPMB) event, 2,600-2,000 M.Y. reactivated the basement rocks, produced amphibolite and granulite facies rocks in the northern and southern blocks respectively and saw the invasion of K-rich granites in the central part of the northern block. A generalised chronology the Karnataka nucleus based on radiometric age data, lithology and fragmentary sedimentologic evidence given by Radhakrishna and Naqvi (1986) is shown in the table 1.1.

It is believed that crustal deformation and thickening gave rise to the EPMB event. The compressional stress directions in the craton and the surrounding mobile belts were E-W, and this produced identical structures in all the regions. (Radhakrishna and Naqvi, 1986). Drury et al., (1984) attributed the general unity of structural features through space and time to the late Archaean shear systems which caused buckling and refolding of the earlier fold belts, making all the linear elements parallel to the direction of shear. Chadwick, et al (1989) studied the facies distribution and structure of Bababudhan - Nallur volcanosedimentary basin and other Dharwar belts and reported that these basins have the characteristics in common with mixed-mode basins developed as a consequence of strike or oblique-slip on long lived fault zones. These authors concluded that plate

interactions comparable with those of the phanerozoic were significant in the late Archaean evolution of south India.

Age (m.y.)	Event
2600	Late Archean
	Invasion of Younger granites (K-rich) bordering the nucleus.  Granulite transformation of older crust along the margins of the nucleus.
3000-2600	Deposition of Younger schist belts (Shimoga, Chitradurga, Sandur).  Conglomerates, orthoquartzites, mafic and felsic volcanic sequences, banded iron formation, greywackes.
	Early Archean
3000	Main development of migmatitic gneisses.
3400	Emplacement of Oldest tonalite - Trondhjemite gneisses with enclaves of ancient supracrustal sequences.
> 3400	Deposition of ancient supracrustal > 3400 Sequences, mafic-ultramafic volcanics and chemical sediments.  Basement predominantly mafic crust.

Table: 1.1. Generalised chronology for the Karnataka Nucleus, After Radhakrishna and Naqvi (1986).

As regards to the origin of metavolcanics of the schist belts Drury (1983) reported that the Metavolcanics of all the schist belts of the Dharwar craton

belonged to a single geochemical group derived from parental magmas generated by shallow angle subduction of the lithosphere. But a recent review on the metabasites of the Dharwar craton (Rajamani,1990) does not indicate the subduction related magmatism to be the root cause for the origin of these rocks, instead a plume related model has been proposed by this author for the metavolcanics of the Dharwar craton.

### **1.3. GOLD MINERALIZATION IN THE SCHIST BELTS OF THE EASTERN DHARWAR CRATON**

The eastern sub block of the Dharwar craton includes the three major auriferous schist belts such as the Kolar, the Ramagiri and the Hutti belts. All the three auriferous schist belts consist dominantly of mafic metavolcanics and they are predominantly tholeiitic in composition, except in Kolar where minor amounts of Komatiitic rocks occur. Felsic volcanics are relatively minor. Kolar and Ramagiri belts also include minor amounts of Banded iron formation. The schist belts are surrounded on all sides by the granitic gneisses. The contact between the schist belts and the gneisses are commonly tectonic. In the Hutti belt, however, an intrusive relation between a late phase granite and the belt rocks have been reported. Detailed and systematic geochemical, geochronological and structural work on the mafic and felsic rocks of the kolar schist belt by krogstad et al (1989) revealed a tectonic "SUTURE ZONE" where two gneiss terranes and atleast two amphibolite terranes with distinct histories were accreted. Based on the

geochemical and isotopic studies on the amphibolites of the eastern and western sides of the Kolar schist belt Rajamani et al 1985., & Balakrishnan et al, 1990 suggested that the volcanic protoliths of the two sides were derived from different mantle sources.

Sivasiddaiah and Rajamani (1989, 1990) carried out a detailed mineralogical and geochemical work on the gold mineralization in the Kolar schist Belt and their studies showed that the sulfide lodes are complex sediments deposited on the seafloor during 2700 ma mafic volcanism and the sediments had a variety of sources including submarine hydrothermal exhalations, seawater and volcanic detritus. These authors also studied the economically important gold quartz vein deposit in the kolar Schist belt, and reported the occurrence of gold in native form in fracture-filled quartz veins hosted by the LREE enriched amphibolites and gneisses.

Zachariah (1992) carried out detailed geochemical studies on the metavolcanics of the Ramagiri gold field and his studies revealed, that the metavolcanics had emplaced in an island arc setting and the belt could be a "tectonic melange". No information is available on the geochemistry of mineralization in the Ramagiri schist belt.

In the Hutti schist belt, only preliminary geochemical data is available on the metavolcanics. (Anantha Iyer and Vasudev 1979, 1980). Based on the limited trace element data, these authors have suggested a marginal basin model for the emplacement of the metavolcanics. Biswas (1990) studied the gold mineralization

in the utiblock of the Hutti schist belt and Classified the gold mineralization into two types viz.,

(1) Syngenetic strata bound type associated with pyritiferous, Carbonaceous schists and (2) Epigenetic lode type hosted by both mafic and felsic rocks. According to this author, the gold mineralization is not structurally controlled in the syngenetic stratabound type and is of little economic significance, where as it is structurally controlled in the Epigenetic lode type which have rich concentrations of gold.

Studies involving gold mineralization should involve a systematic geochemical, structural, isotopic and field studies, and should be concerned with what we know about gold deposits and what we need to know. Our understanding of the gold mineralization can be summarised as follows.

1. Gold deposits appear to have formed by multistage enrichment processes.
2. There seems to no mineralogical control, since gold occurs by itself in the native state.
3. Higher concentrations of gold are reported from Archaean greenstone belts all over the world.
4. Palaeozoic gold deposits are reported from collision tectonic zones/convergent plate boundaries.
5. It is not a magmatic deposit. It is a hydrothermal deposit formed from hydrothermal solution. Although it is hydrothermal, it does not seem to be associated with other class of hydrothermal deposits, Wherein the basemetals occur. So probably it requires a unique hydrothermal system of formation and deposition.



Based on our present knowledge, we can classify the gold deposits into two broad categories.

- (i) Vein quartz gold associated with metavolcanics.
- (ii) Stratiform sulfide Lode associated with iron formation.

The vein quartz gold deposits are epigenetic in origin and the veins themselves are localised in shearzones in metabasaltic rocks in collision tectonic Zones. On either side of the vein carbonate and/or Biotite alteration is seen. The environment of deposition could be such that the water/rock ratio was low, ie., a small volume of fluid passed through a large volume of rock eventually got channelised and could have given rise to a focussed flow and a drop in temperature and changes in the Eh-Ph conditions could have caused the deposition of gold.

The stratiform type gold deposits associated with sulfide facies of the iron formation is of syngenetic origin because the Chemistry of the iron formation and the Chemistry of the Orelodes are the same. (Siddaiah et al, in preparation). Gold is found in sulfide lenses which are parallel to the iron formation, and the iron formation itself is associated with volcanics. Syngenetic sulfide lode deposits of gold are relatively minor in amount and are of little economic significance.

Detailed geochemical studies have to be done on the epigenetic vein quartz gold deposits to understand the details about (i) source for fluids ? (ii) source for gold ? (iii) Rock type which is important for the gold mineralization (iv) what aspect to the Rock type is important ? ie., whether it is the major element Chemistry or the trace elements which controlled the mineralization and (v) The structural

aspects/tectonics responsible for gold mineralization. It is possible that a combination of these factors would have given rise to gold mineralization. A critical evaluation of the above mentioned questions will be useful for future gold exploration.

## **CHAPTER 2**

### **HUTTI - AREA OF STUDY**

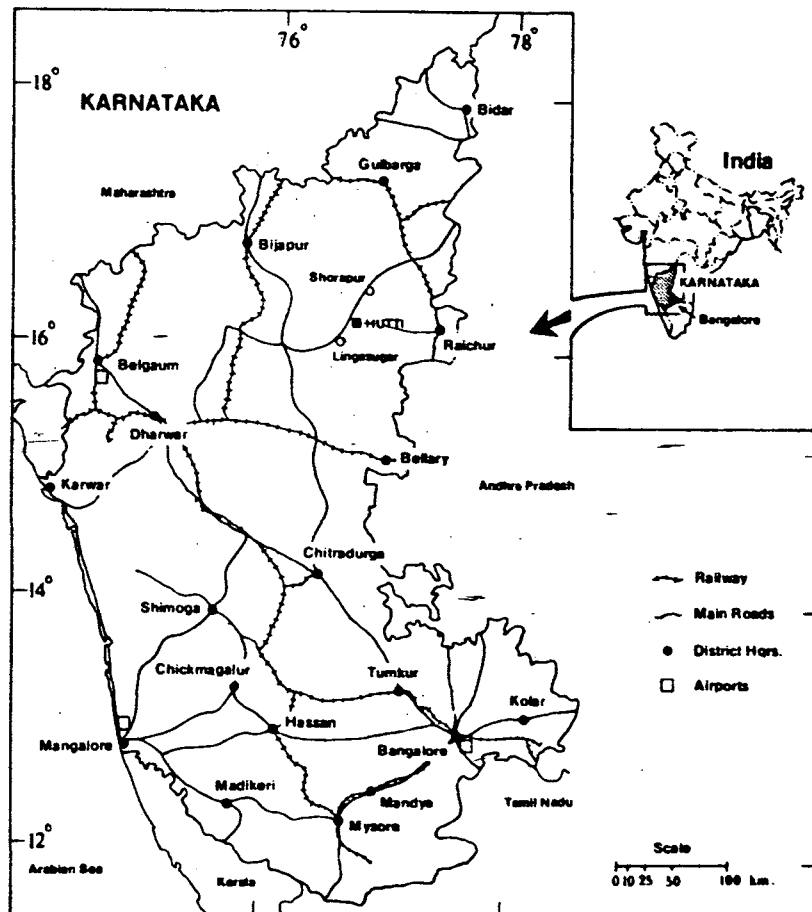
#### **2.1 : LOCATION AND ACCESSIBILITY**

The Hutti gold field takes its name from the village of Hutti (Lat. 16°12'N, Long. 76°43'E). The area under investigation is the hook shaped schist-belt shown in the fig. 2.2, falling within the Raichur District, Karnataka. Hutti is some 480 km north of the state capital of Karnataka, Bangalore, and about 80 km west of Raichur, the district head Quarters and about 10 km (by road) east of Lingusugur, the taluk headquarters. It is connected to all parts of the State by all-weather roads.

The nearest railhead is raichur, and the area has full public transport, postal, telephonic, telegraphic and banking facilities.

#### **2.2 PHYSIOGRAPHY AND CLIMATE**

Hutti is almost central in the Deccan plateau, midway between the Western and Eastern Ghats. The topography is generally flat, but with numerous conspicuous granite out crops of Considerable height. The area is largely covered by black cotton soil, often of considerable depth. The elevation above sea level is about 523 meters.



Location map of Huttu, Karnataka.

Average rainfall is about 500 mm received mostly during the S.W. monsoon period (June - September) and maximum and minimum temperatures are about 40°C and 10°C respectively. Being an open area, temperatures fall rapidly after sunset.

### **2.3 PREVIOUS WORK**

Most of the work undertaken at the Hutti gold mines before 1970 were unpublished reports prepared by the organisations involved in the mining and exploration of gold. The first available published information is provided by Vasudev V.N. and Naganna C. (1973). These authors have recognised three distinct stages of mineralisation in the gold-Quartz-Sulfide reefs of Hutti gold mines. According to them, the minerals formed during first stage are rutile, pyrite (with traces of gold), arsenopyrite, quartz (reef and vein type) and carbonates. Minerals of the second stage are Pyrrhotite, chalcopyrite, sphalerite, galena and gold. Minerals of the third stage are pyrite, calcite, and quartz formed along numerous minor faults (slips) and major faults. These authors have also recognised three generations based on the textural and associational criteria viz., (1) Gold-Pyrite association (2) Gold-arsenopyrite-quartz association and (3) Gold-sphalerite-quartz association, and concluded that only the gold of the second and third generations constitute the lode.

Ziauddin, M. and Narayanaswamy S., (1974) and Mahanty S.C., and Raju K.K. (1974) Studied the structural features which controlled and localised the gold

quartz mineralisation in Hutti and considered them to be enechelon shear fractures, drag folds and late fractures.

Ramakrishnan et al (1976) classified the Hutti- Maski schist belt under the keewatin type.

Abhinaba Roy (1979) recognised polyphase folding deformation in the Hutti schist belt. This author has reported three phases of folding deformation ( $F_1$ ,  $F_2$  and  $F_3$ ) and concluded that the gold mineralisation is controlled by first phase of folding ( $F_1$ ) and the associated greenschist facies Metamorphism on the regional scale.

Anantha Iyer and Vasudev (1979) and Anantha Iyer et al. (1980) have studied the Metabasalts for major elements and REE by spark source mass spectrometry. Based on the limited data on trace Elements, these authors have suggested a Marginal Basin Model for the emplacement of these volcanics.

Safonov et al (1980) have done fluid inclusion studies on the auriferous quartz of Hutti and reported both primary and secondary fluid inclusions similar to those of quartz of "Champion Reef" (Kolar Gold Field). According to these authors, the primary fluid inclusions are of two phase variety - gas and liquid which occurs in the ratio of 1:6 and that these phases homogenise into a liquid phase at a temperature of 130°C-150°C.

Abhinaba Roy and K.K. Raju (1980) reported the occurrence of an olivine dolerite dyke which is said to cut the metabasalts of Hutti and the associated granites and showing somewhat unusual Chemical composition with 17% Olivine in the norm.

Biswas et al,(1985),have studied the mineralization, rock types, structure and

metamorphism of the Hutti gold fields, the extract of which is given in the next section of this chapter under the title "Geology of the Hutti Schist belt".

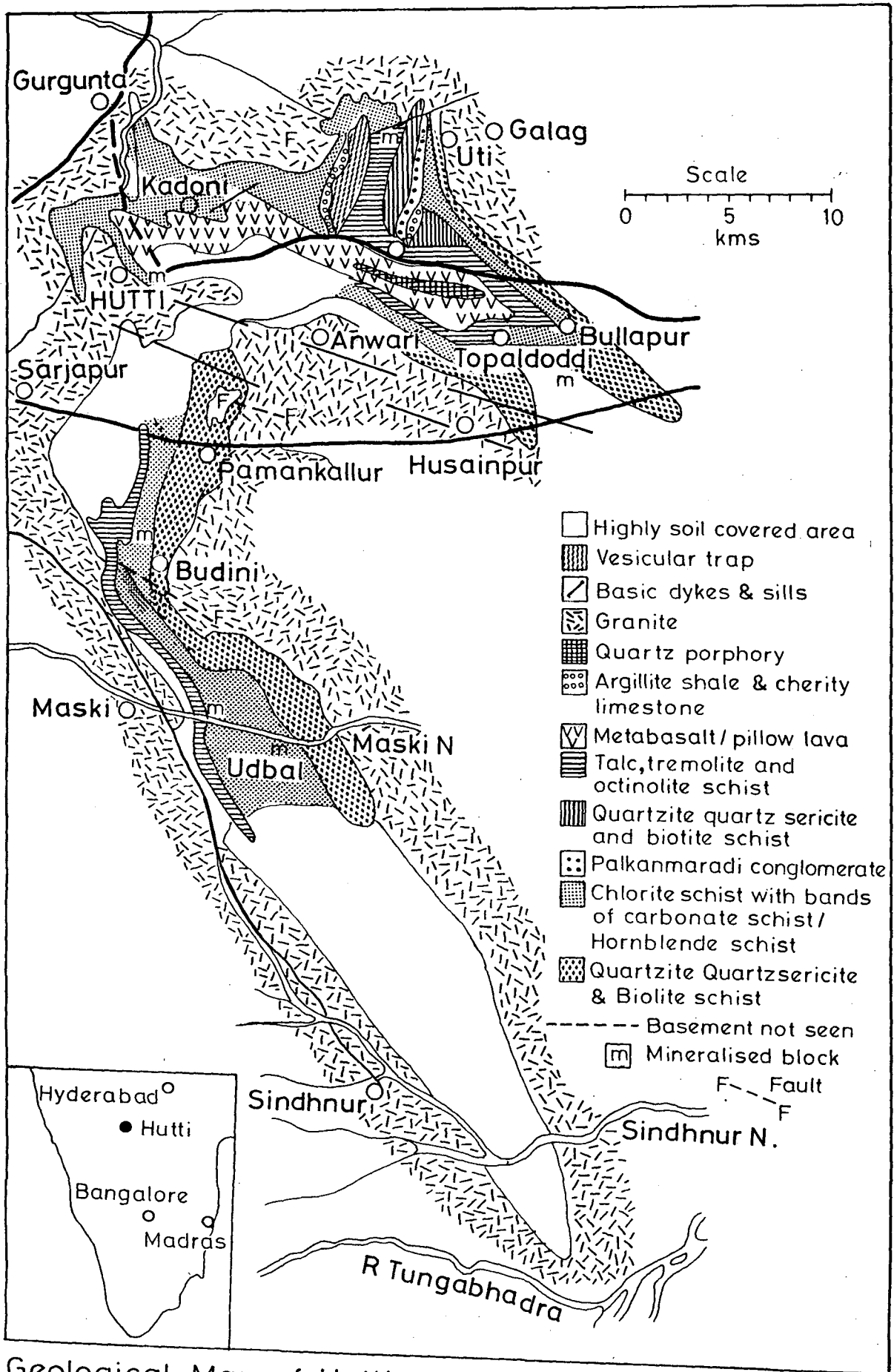
Sarkar (1988) reported scheelite mineralisation in three of the six working lodes in the Hutti gold Mines.

L.C. Curtis et al., (1990) have studied the geology and structure of the various lithounits and said that the rock units have undergone three phases of folding, the first two of them ( $F_1$  and  $F_2$ ) being Coaxial isoclinal folds.

Biswas (1990) classified the gold mineralization in the recently developed utiblock of the Hutti-Maski supra crustal belt into two groups viz., (1) syngenetic stratabound type and (2) Epigenetic lode type. According to this author, the syngenetic stratabound type mineralisation is confined to the Pyritiferous carbonaceous schist and has little economic significance when compared to the Epigenetic lode type mineralization which is hosted by both mafic and felsic units.

## **2.4 GEOLOGY OF THE HUTTI-MASKI SCHIST BELT**

The Hutti schist belt is a volcanic-dominated Archaean greenstone belt covering an area of 750 km<sup>2</sup> in the eastern block of the Dharwar Craton. It is a hook-shaped belt about 65 kms in length and about 8 kms in width. The geological map of the Hutti-Maski schist belt given by Curtis et al., (1990) is given in the fig. 2.2.



Geological Map of Hutti-Maski Schist Belt Karnataka, India. (redrawn after Biswas et al. 1985)



The following account of the regional geological set up is extracted from Biswas, et al (1985) :

"The Hutti-Maski schist belt Consists predominantly of a volcanic suite of rocks (90 to 95%) with subordinate Metasedimentaries. Pillow bearing basaltic rocks dominate the volcanic suite and are followed in frequency by acid to intermediate lavas and quartz/rhyolite porphyry. Terrigenous sedimentaries are exposed in the eastern part of the belt, represented by andalusite - bearing mica, schist garnet-Cordierite gneiss and garnetiferous Mica schist. The schist belt is surrounded on all sides by granitoids which show intrusive relationship in majority of the places. Although there is no direct evidence to say that some of them are basement the presence of a conglomerate horizon within the schist belt with well rounded pebbles and boulders of tonalite gneiss suggests a pre-existing sialic crust. A number of small granodiorite bodies are seen over various parts. The effect of granitisation is a common phenomenon along the eastern margin, manifested by the development of migmatites. The last igneous activity is manifested by quartz and pegmatite veins and dykes of dolerite and gabbro.

#### **2.4.2 STRUCTURE OF THE HUTTI GOLD FIELD**

The rocks of the Hutti schist belt have undergone three distinct phases of folding deformation, henceforth referred to as HuD<sub>1</sub>, HuD<sub>2</sub> and HuD<sub>3</sub>. HuD<sub>1</sub> is characterised by the development of microscopic and mesoscopic folds of the first phase which are isoclinal in nature, concentric in geometry, and enechelon in pattern

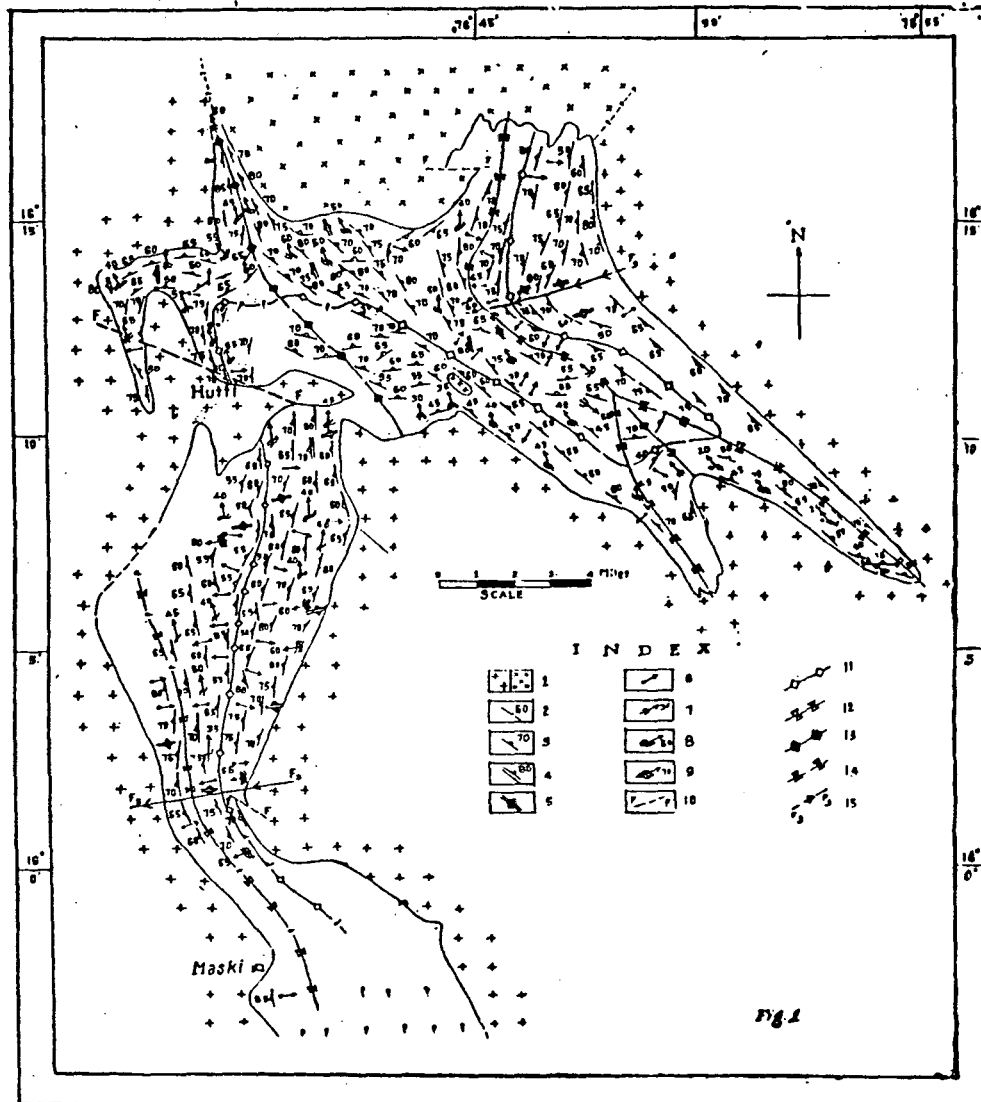
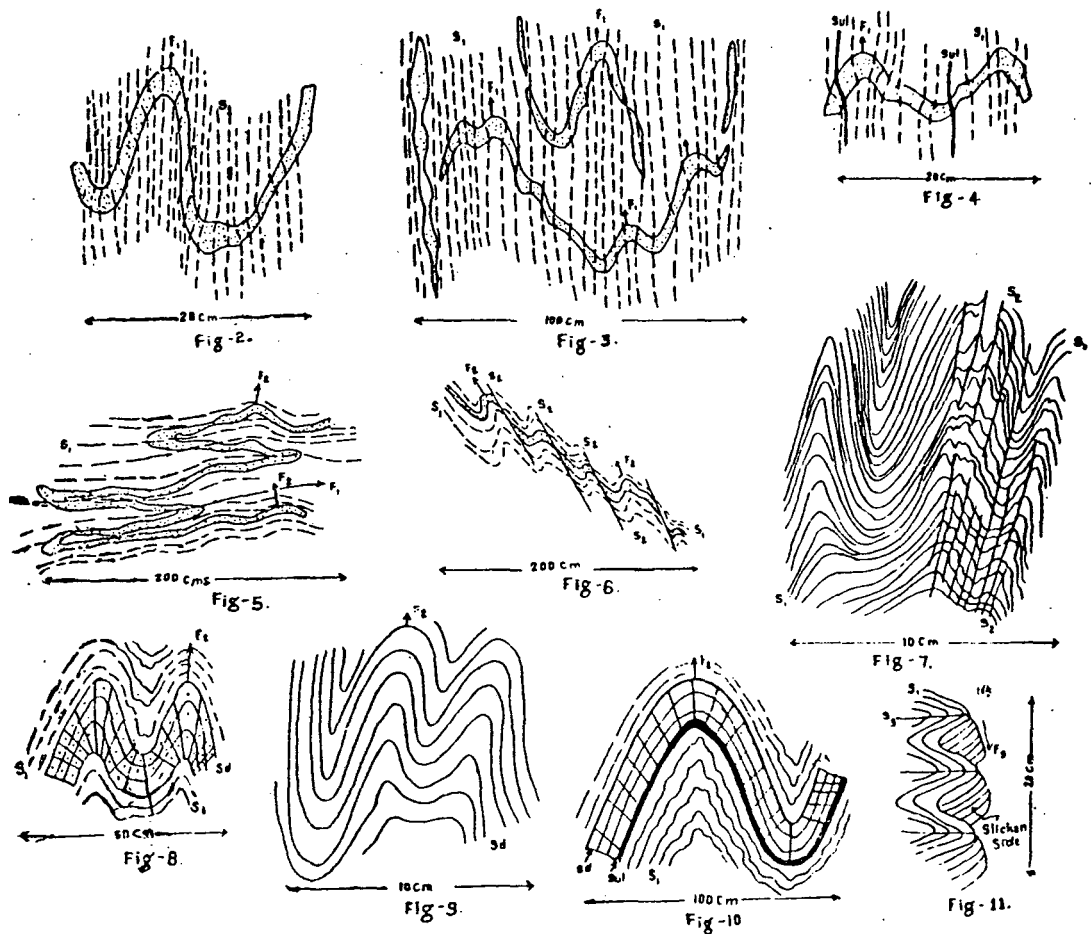


Figure 1. Generalised structural map of the Hutti-Maski schist belt. Boundary of the schist belt was taken from the original map done by Ramaswamy and Krishnamurthy (1968). Index: 1. Granodiorite/granite. 2. Bedding plane ( $S_0$ ). 3. Schistosity ( $S_1$ ). 4. Crenulation cleavage ( $S_2$ ). 5.  $S_3$  Cleavage. 6. Pillow showing top direction. 7.  $F_1$  minor fold axis. 8.  $F_2$  minor fold axis. 9.  $F_3$  minor fold axis. 10. Probable fault. 11.  $F_1$  anticlinal axial trace. 12.  $F_1$  synclinal axial trace. 13.  $F_2$  antiformal axial trace. 14.  $F_2$  synformal axial trace. 15.  $F_3$  axial trace.

Fig. 2.3. After Abinaba Roy, (1979)



- Figure 2.  $F_1$  minor fold in vein quartz (stippled), showing cleavage ( $S_1$ ) refraction. Wandalli.
- „ 3. Development of  $F_1$  minor fold as well as boudin or pinch and swell structure in vein quartz (stippled) in the same exposure. Topaldari.
- „ 4. Sulphide (Sul) vein concordant to schistosity ( $S_1$ ). Madarinkota.
- „ 5. Refolded fold in vein quartz (stippled). Madarinkota.
- „ 6. Crenulation or slip cleavage ( $S_2$ ) developed on vein quartz (stippled) and schistosity ( $S_1$ ) Madarinkota.
- „ 7. Zonal development of crenulation cleavage ( $S_2$ ). Kadoni.
- „ 8.  $F_2$  fold on mylonite band ( $S_4$ ) and schistosity ( $S_1$ ) and development of radial fractures in folded vein quartz. Hutti Gold Mine.
- „ 9. Near concentric  $F_2$  fold on mylonite band ( $S_4$ ) in gold quartz vein, Hutti Gold Mine.
- „ 10.  $F_2$  fold on sulphide (Sul) vein.
- „ 11. Slickensides developed perpendicular to  $F_3$  fold axis, East of Pamankallur.

Fig. 2.4. After Abinaba Roy, (1979)

and of penetrative planar structure defined by preferred orientation of neomineralised chlorite, biotite and hornblende. Flattening of quartz grains is syntectonic with  $HuD_1$ .

$HuD_2$  shows the development of minor and macroscopic folds of second generation which are both tight and open in nature, concentric in geometry and are characterised by the development of crenulation cleavage.  $HuD_3$  is marked by the presence of Kink folds. The first two deformations were pronounced and the regional tectonic manifestation of the schist belt is represented by these fold movements.

During the first deformation ( $HuD_1$ ), the rocks were thrown into NNW-SSE trending isoclinal antiforms and synforms. The present Hookshape of the schist belt is due to refolding of the first deformation on NW-SE axis of  $HuD_2$ . The third deformation ( $HuD_3$ ) shows broad warps on regional scale on an East-West axis.

The generalised structural map and diagram showing various structural features of the Hutti-Maski schist belt given by Abinaba Roy (1979) are shown in the figures 2.3 and 2.4.

#### **2.4.3 METAMORPHISM OF THE HUTTI SCHISTBELT**

The rocks of the schist belt have undergone upto amphibolite facies of regional metamorphism having a relationship with the phased deformational episodes. During  $HuD_1$ , the rocks attained greenschist to amphibolite facies metamorphism with a general increase in the metamorphic grade from south to North.

TH-4558



The mineralised zones marked by chlorite and biotite are due to retrogression of amphibolite at a later stage of the same deformation  $HuD_1$  and related to wall rock alteration during mineralization. The second deformation ( $HuD_2$ ) does not show any neomineralization. The third deformation shows the effect of retrogression at places where the hornblende breaks down to chlorite along the hinge zones of the  $HuD_3$  folds.

## **2.5 FIELD OBSERVATIONS**

The mafic rocks of the Hutti schist belt include predominantly the metabasalts which are now represented by different textural varieties of amphibolites and chlorite schist. Important locations where good outcrops of both mafic and felsic rocks are present and hence field observations have been made include Wondalli, Palkanmardi, Madriankota, Uti, Pamankallur and Gurgunta. The hook shaped schist belt is bounded on all sides by the granitoids which in general have sharp tectonic relation with the mafic rocks. (Fig. 2.5). However in the northern part of the schist belt, near the Uti village, one phase of leucocratic granite cross cuts the metabasalts and include large xenoliths of the latter. (Fig. 2.6). In many places the contact is covered by soil developed from sheared lithologies. The mafic rocks in the eastern contact are of higher metamorphic grade (middle to upper amphibolite facies) represented by well recrystallized amphibolites and that on the western contact are of a relatively lower grade represented by the chlorite-carbonate schist. In the pamankallur area, good exposures of well foliated

metabasalts are seen. The metabasalts of this area have undergone low grade metamorphic alteration and are now represented by the chlorite schist. There are quartz and carbonate veins in the Chlorite schist and the Quartz veins show the development of pinch and swell structures, indicating that the deformation continued beyond the vein formation. There are both dextral and sinistral shearing in the metabasalt and the shear planes are smeared with muscovite in this area. Specks of Sulfide minerals like pyrite, arsenopyrite etc are present in the chlorite schist. At the western contact, the rocks are highly sheared and both mafic and felsic rocks are pulverized. Spheroidal weathering is also seen in the pamankallur area.

In the chinchargi village the metabasalts show evidence of folding and shearing deformation. South of Chinchargi village, two textural varieties of metabasalts viz., the finegrained massive amphibolite and coarse grained spotted variety are seen. The finegrained metabasalt are well foliated and show  $F_3$  type open folds and the orientation of the axialplane of the fold is  $N15^\circ E$  (Fig. 2.7). Pillow structures with cherty layers caught up in them are seen in this area. The coarse grained amphibolite is juxtaposed with the fine grained amphibolite with sharp lithological boundary. An acid volcanic unit represented by the Quartz porphyry is seen. This rock is medium grained consisting of bluish grey Quartz as the dominant mineral and is well foliated and two sets of foliation giving rise to an anastomosing appearance is seen on the weathered surface. Foliation is not seen on the fresh surface. The trend of the main foliation is  $N30^\circ E$  which is parallel to the strike of the rock. The dip of the foliation surface is almost vertical.

In the Madriankota village, the metabasalts are represented by the medium grained schistose amphibolite. The trend of the foliation in this area is E-W and the dip of the foliation surface is  $75^{\circ}$  due North. North of Madriankota village, in the riverbed good exposures of the metabasalt and granite are seen. The contact of the metabasalt with the granite is sharp and tectonic. The rocks on either side of the contact are mylonitised and mylonitic banding is prominent in the metabasalt.

In the wondalli area, the rocks are mainly intermediate to acid volcanics which are unaltered, very finegrained, and well foliated. The trend of the foliation is almost east-west. Mineral lineations are present in the mylonitised acid volcanics and they are steeply dipping in the southern direction. Epidote veins are present along the sub-horizontal fractures in the acid volcanics.

In the palkanmardi area, in the north eastern part of the schist belt, a conglomerate horizon with well rounded pebbles of granitic composition embedded in a darker finegrained matrix is seen. The clastic pebbles are rounded and at places are stretched/elongated. (Fig. 2.9). This may be due to varying degrees of deformation that the rocks must have undergone. The pebbles are stretched parallel to the foliation of the matrix and the pebbles themselves have gneissic foliation. This conglomerate unit appears to be similar to champion gneiss occurring in the eastern margin of the kolar schist belt. (S. Balakrishnan and V. Rajamani, 1987).

In the Uti area, which represents the northernmost part of the Hutti schist belt, the metabasalts are represented by finegrained and coarse grained amphibolites. The finegrained metabasalts are well foliated and there are tongues

of leucocratic granite in the metabasalts which indicates an intrusive relationship in this area.

### Summary of field observations

From the field observations it is evident that the mafic rocks of the Hutti schist belt include predominantly the metavolcanics. The metavolcanics of the Huttishist belt ranges in composition from basic to intermediate and acid volcanics and hypabyssal intrusions represented by the Quartz porphyry. At some places, near Pamankallur the metabasalts appear to be volcanoclastics.

The metabasalts are now represented by three textural varieties of amphibolites namely (i) the coarse grained spotted amphibolite (ii) Fine grained massive amphibolite which are mylonitised, and (iii) Medium grained schistose amphibolite. The metabasalts are commonly well foliated and in many places two sets of foliation, one cutting the other at a lower angle giving rise to an anastomosing appearance is seen. This eventually leads to the development of lozenge shaped bodies in the field. The fine-grained metabasalts show pillow structures with cherty layers in them indicating that their protoliths are emplaced under subaqueous conditions. The coarse grained amphibolite which occurs as a continuous band within the fine grained amphibolite with sharp lithological boundary can be interpreted as synvolcanic gabbroic sills. The rocks of the Hutti schist belt have undergone one or more episodes of folding deformation followed by brittle to



brittle-ductile shearing and the sense of shear movement is both dextral and sinistral. Metamorphism in the Hutti schist belt increases from south to North. This is supported by the presence of low grade rocks like Chlorite Carbonate schist in the southern part and well recrystallized amphibolites in the northern part. The presence of a conglomerate horizon with pebbles of granitic composition embedded in a finegrained matrix points to the ensialic tectonic setting for the rocks of the schist belt.

## **2.6 PETROGRAPHY**

### **1. Sample No: GH -3**

**Location** : Wondalli Road

**Megascope Identity** : Fine to medium grained rock, mesocratic, consisting of amphiboles, quartz and plagioclase with incipient foliation.

**Microscopic Identity** : It is a finegrained rock with well developed schistose foliation. Segregation of mafic minerals from the felsic minerals is seen. The quartz and plagioclase are crushed and granulated. Chloritization of biotite is seen.

**Modal percentage** :

Actinotite = 45% Quartz = 30%

Plagioclase = 15% Biotite = 4% Chlorite = 1%

Opaques = 4-5%

**Texture** : schistose, cataclastic.

Rock type : Diorite (?)

2. Sample No : GH -4

Location : South of Chinchargi

Megascope Identity : It is a coarse grained spotted variety of amphibolite, mesocratic to melanocratic, without foliation.

Microscopic Identity : The rock under thin section has a metamorphic fabric with two sets of foliation. Individual amphibole grains are granulated giving rise to a Patchy extinction under the microscope (fig. 2.9). It appears that the rock has undergone probably a high degree of brittle deformation at a lower grade of amphibolite facies metamorphism. The Al content of this rock (15 Wt%) indicates that the amphiboles are of Pargasitic composition.

Modal percentage : Actinolite = 65% Hornblende = 10%

Plagioclase = 10% Quartz = 10%

Opaques = 5%

Texture : schistose, cataclastic

Rock Type : AMPHIBOLITE

SAMPLE NO : GH -5

LOCATION : South of chinchargi

Megascope Identity : It is a finegrained rock with a mylonitic banding consisting of amphiboles, plagioclase and quartz.

Microscopic Identity : The rock under thin section has a strong metamorphic fabric with well developed schistose foliation (2 sets), Consisting mainly the fibrous

aggregates of actinolite, and Hornblende with little plagioclase and quartz.

Modal percentage : Actinolite = 45% Hornblende = 25%

Quartz = 15% Plagioclase = 10%

Opaques = 4-5%

Texture : schistose, fibrous.

Sample : GH-7

Location : Palkanmardi

Megascope Identity : It is a melanocratic, medium grained schistose rock consisting mainly of amphiboles, with little plagioclase feldspar and quartz.

Microscopic Identity : The rock under thin section is a highly recrystallized schistose rock consisting mainly of Hornblende (80%) little plagioclase and quartz. There are 2 generations of Hornblende, one of which is slender and Prismatic in habit while the other is an euhedral hornblende (enclosed in the prismatic variety) (fig. 2.13). The Euhedral hornblende could be of younger generation formed probably due to reheating by the nearby granitic intrusion. The higher amounts of hornblende (>80%) could be explained by a reaction involving precursor pyroxene and plagioclase giving rise to Hornblende + Quartz + ilmenite.

Pyroxene + plagioclase + H<sub>2</sub>O --> Hornblende + Quartz + Ilmenite.

The higher amount of opaques is also explained by the above reaction, by way of ilmenite in the product.

Modal percentage : Hornblende = 75% plagioclase = 5%

Quartz = 10% Biotite = 2% Opaques = 7%

Texture : schistose

Rock Type : Amphibolite

Sample No : GH -8

Location : Madriankota Riverbed, Western side of the Road

Megascopic Identity : It is fine grained mesocratic rock consisting of amphiboles, plagioclase and little epidote, without foliation.

Microscopic Identity : It is a finegrained, with an incipient schistose foliation, consisting of hornblende, actinolite, Zoisite, clinozoisite, Quartz and little Epidote.

The calcic Plagioclase has been altered to zoisite/clinozoisite during retrograde metamorphism.

Modal percentage : Hornblend = 60%

Clinozoisite = 20% Quartz = 15% Epidote = 3-4%

Texture : schistose

Rock Type : AMPHIBOLITE

Sample No : GH -10

Location : Madriankota River bed, Eastern side of the causeway.

Megascopic Identity : It is a medium grained, melanocratic well foliated rock consisting of amphiboles and plagioclase. Microscopic Identity : It is a well

recrystallized, medium to coarse grained rock with well developed schistose foliation consisting mainly of Hornblende, actinolite, plagioclase, Quartz and little clinozoisite and opaques. Hornblende has inclusions of Quartz and feldspar.

Modal percentage : Hornblende = 50% Actinolite = 15%

Plagioclase = 10% Quartz = 10% Clinozoisite = 4%

Opaques = 4%

Texture : schistose, porphyroblastic

Rock Type : Amphibolite

Sample No : GH -11

Location : East of chinchargi

Megascope Identity : It is a coarse grained spotted variety of amphibolite consisting mainly of hornblende and plagioclase.

Microscopic Identity : The rock under this section has a metamorphic fabric with 2 sets of foliation. The quartz and feldspar are granulated and form the matrix with hornblende porphyroblasts as "augens" in them. The rock is variably deformed. Hornblende has bent cleavages. The hornblende augens could have developed as a result of shearing in two directions at small angles (fig. 2.11). The plagioclase grains swerving around the hornblende augens is seen.

Modal percentage : Hornblende = 60% Quartz = 20%

Plagioclase = 15% Opaques = 4-5%

Texture : schistose, cataclastic, porphyroblastic

Rock Type : Amphibolite

Sample No : GH -12

Location : East of Chinchargi

Megascope Identity : It is a finegrained, equi-granular rock with well developed foliation, mesocratic consisting of amphiboles and plagioclase.

Microscopic Identity : The rock under thin section is finegrained with incipient foliation. The orientation of amphiboles is somewhat chaotic. Quartz and feldspar are granulated. Some of the calcic plagioclase have been altered to clinozoisite.

Modal Percentage : Hornblende = 65% Actinolite = 5%

Plagioclase = 10% Quartz = 10%

Clinozoisite = 5% Opaques = 5%

Texture : Schistose, Cataclastic

Rock Type : Amphibolite

Sample No : GH -13

Location : Near pamankallur, on the western side of the Hutti - pamakallur Road.

Megascope Identity : It is a finegrained schistose rock with 2 sets of foliation, giving rise to an anastomosing appearance. The rock consists of light green coloured minerals which may be amphibole or chlorite, Plagioclase feldspar and specks of sulphide minerals.

Microscopic Identity : The rock under thin section has fine grained Chlorite, Calcite, Quartz, Plagioclase and opaques with well developed schistosity. Even the opaques

are aligned in one direction, indicating high stress conditions. Calcite grains are crushed and pulverized giving a smudgy appearance, which may be due to another period of deformation, after the vein formation.

Modal percentage : Chlorite = 55% calcite = 30%

Plagioclase = 6% Quartz = 5% Opaques = 2-3%

Texture : schistose

Rock Type : Chlorite - carbonate schist

Sample No : GH -14

Location : Near pamankalur MECL Camp, on the southern side of the P. Kallur - Gurgunta Road.

Megascope Identity : It is a mesocratic, finegrained massive rock without foliation, consisting of amphiboles, plagioclase and Quartz.

Microscopic Identity : The rock under thin section has a metamorphic fabric, consisting of hornblende, actinolite, Quartz, Plagioclase, carbonates, clinozoisite and opaques. The actinolite occurs as fibrous aggregates (fig. 2.14). The calcic plagioclase alters to Clinozoisite.

Modal percentage : Actinolite = 55% Carbonates = 10%

Quartz = 15% Plagioclase = 15%

Clinozoisite = 2% Opaques = 2-3%

Texture : Schistose

Rock Type : Amphibolite

Sample No : GH -16

Location : On the Southern side of the Paman Kallur - Gurgunta Road 2 Kms from P. Kallur.

Megascope Identity : It is a finegrained massive rock without foliation. It gives effervescence with dil. Hcl. It consists of chlorite, and carbonates.

Microscopic Identity : The rock under thin section is a medium grained, inequigranular rock with incipient foliation and Contains chlorite, calcite and quartz. The Calcite grains give a smudgy appearance probably because of recrystallization.

Modal percentage : Chlorite = 40% Calcite = 35%

Quartz = 15% Opaques = 5% Feldspar = 5%

Texture : Medium grained, inequigranular, weakly schistose.

Rock Type : Chlorite carbonate Rock

Sample No : GH -17

Location : Same as that of GH -16, at the western contact

Megascope Identity : It is a finegrained, mesocratic equigranular rock without foliation, containing amphiboles and plagioclase.

Microscopic Identity : The rock under thin section has an igneous texture with plagioclase laths forming the matrix and clinopyroxene as phenocrysts in them (fig. 2.18). The phenocrysts have been altered to actinolite by Static metamorphism and that is followed by fluid alteration by which the actinolite has been converted into Biotite. The Ca and Al released as a result of this fluid alteration goes to makeup



the Epidotes.

Modal percentage : Actinolite = 55% Plagioclase = 20%

Clinopyroxene = 5% Biotite = 8% Epidote = 5%

Quartz = 7%

Texture : relict Igneous, sub ophitic, subpoikilitic

Rock Type : Metabasalt

## **CHAPTER - 3**

### **ANALYTICAL PROCEDURES**

#### **INTRODUCTION**

Deducing valuable information from geochemical data requires accurate and precise determination of the concentration of the elements present in the samples under consideration. The quality of geochemical data should be such that a meaningful interpretation can be made out of it. Maximum care was taken throughout the data acquisition process to obtain data of precision.

#### **3.1 SAMPLE PROCESSING**

About 2-3 kg of freshest rock possible samples were collected and reduced to small chips in the field itself. While collecting the samples, veins and other inhomogenities were removed from the sample and about 500 gms of the homogenised sample was crushed in a hardened steel mortar to 60 mesh size. From this crushed sample 100 gram was collected by coning and quartering method and was ground to -200 mesh size in an agate mortar. This -200 mesh size powder were stored in plastic vials and the same was used for the preparation of sample solution. Once the sample was ground to -200 mesh size, the steel mortar and pestle and the agate mortar, the sieves and other accessories were washed with soap solution, dried up and then cleaned with acetone before proceeding to the next sample, thereby limiting the inter-sample contamination.

## 3.2 SAMPLE DISSOLUTION

### 3.2.1 Preparation of "B"-Solution :-

"B"-Solution is prepared by acid digestion method using concentrated  $\text{HNO}_3$  and Conc. HF acids. This solution was used to analyse all the elements except Si, and Zr. The procedure used in this work is a modified method of Shapiro and Brannock (1962).

About 0.5 g of sample powder (-200 mesh) was taken in a cleaned teflon crucible. To this 10 ml of conc. HF and 5 ml of conc.  $\text{HNO}_3$  were added and was heated at a temperature of  $90^\circ\text{-}100^\circ\text{C}$  with the lid on for about 4 hours in a hot plate. After 4 hours, the lid was removed and was heated to dryness. In the second phase, 5 ml of conc. HF and 10 ml of conc.  $\text{HNO}_3$  were added and then evaporated to dryness. In the third phase, 5 ml conc.  $\text{HNO}_3$  was added and again evaporated to dryness. Finally, 20 ml of 1N HCl was added and was heated to  $100^\circ\text{C}$  to bring the digested sample into solution. After regular swirling, the solution was transferred to a 100 ml volumetric flask and was made up to the volume with the help of triple distilled water. Thus, a 200 times diluted rock solution was prepared. This solution was directly used for trace element analyses except Zr, and an aliquot of this solution which was diluted 25 times more (5000 x) was used for major element analyses except Na and K. For Na and K 2000x diluted solutions were used.

### 3.2.2 GRAVIMETRIC DETERMINATION OF SILICA BY ALKALI FUSION

Several alkali salts are extremely efficient at dissolving silicate rocks and melt at lower temperatures. In this method of determination of silica, NaOH Pellets, and  $\text{Na}_2\text{O}_2$  Powder were used.

About 1 g of NaOH and 1.25 g of  $\text{Na}_2\text{O}_2$  were weighed in a metler 240 digital balance and transferred to a pre cleaned Nickel crucible. To this 0.5 g of sample powder (- 200 mesh) was accurately measured and transferred to the Ni-crucible in such a way that the sample does not touch the walls of the crucible. Thus the sample to flux ratio was 1:4.5.

The Ni-crucible is then covered with a lid and fused over a meker burner for about 20 minutes, till the red hot condition of the crucible bottom is reached. The crucible was then cooled for about 30 minutes and 25 ml of triple distilled water was added and allowed to stand covered overnight. The contents of the Ni-crucible were then transferred to a beaker. The crucible and the lid are washed down completely with 40-50 ml of 6N HCl and a teflon rod is used to scrap out the material sticking to the wall of the crucible, and then again rinsed with 6N HCl and transferred to the beaker. The solution thus collected in the beaker was kept on a hot plate and heated to near dryness.

The residue is dissolved in 100 ml 1N-HCl when silica precipitates while all the other elements are taken into solution. The solution with the silica precipitate was then passed through a filter paper in a funnel attached to a filtration flask - vacuum pump setup. The filtered material in the funnel was washed down repeatedly with triple distilled water, so that all the other elements except silica

goes into the filtrate. The final filtered material consisting of silica should be colourless. If it is coloured, then it means that coprecipitation of some other elements has taken place.

The silica precipitate in the filter paper was then transferred to a pre-cleaned platinum crucible and covered with the lid and kept in a muffle furnace at 900°C for about 45 minutes. The platinum crucible is then removed, cooled for a minute and then kept in a vacuum desiccator, so that it does not absorb moisture. The silica ash is then weighed in a balance accurately and the value obtained is multiplied by two and then converted into percentage.

Accuracy of the silica values obtained by this method was checked out with the help of an internal rock standard MB-H. The silica value reported for this rock standard is 49.5% and the value obtained by this method was 49.2%. So the accuracy of this method is considered to be good.

### **3.2.3 Preparation of Sample Solution by $\text{LiBO}_2$ - fusion**

In this method 0.2 g of the sample powder is fused with 0.8g of  $\text{LiBO}_2$  in a Pre-ignited and cleaned graphite crucible. The sample powder was added in such a way that it does not touch the crucible walls, since it was found that the fused material has a tendency to stick to the walls in such cases. The mixture was then heated in a muffle furnace from 800°C to 1050°C in an hour and allowed to remain at 1050°C for 10 minutes. The fusion cake was then poured into a teflon beaker containing 35 ml of 2N  $\text{HNO}_3$  and kept on a magnetic stirrer for about 45 minutes till the fused material completely goes into solution. The Solution thus obtained

were made up to volume in a 50ml volumetric flask and the solution was used directly for the analysis of Zr.

Table 3.1 : Analytical wavelengths, nature and concentration of solutions used for analyses. All analyses by ICP-AES except Na and k by Flame Photometer.

Element	Wavelength Used	Solution	Concentration
Si	-	Gravimetric	-
Ti	336.121	"B"	5000 x
Al	396.152	"B"	5000 x
Fe	259.940	"B"	5000 x
Mg	279.553	"B"	5000 x
Mn	257.610	"B"	5000 x
Ca	317.933	"B"	5000 x
Na	588.995	"B"	2000 x
K	766.500	"B"	2000 x
Ni	231.604	"B"	200 x
Cr	267.716	"B"	200 x
Ba	455.403	"B"	200 x
Sr	407.771	"B"	200 x
Zr	339.198	LiBO <sub>2</sub>	250 x

### **3.3. ANALYSIS OF MAJOR AND TRACE ELEMENTS BY ICP-AES**

#### **3.3.1 The Instrument**

The instrument used for the analysis is a Labtam 8440 model manufactured by Labtam Limited, Australia, fitted with a monochromator for sequential analysis of elements and a polychromator for the Simultaneous determination of 10 REES. The wave lengths used for the operation are listed in the Table.3.1.

In terms of sensitivity, speed of analysis and capability for both major and trace element determinations, the ICP-AES has brought wet chemical schemes of analysis into the league of other established instrumental techniques such as XRF, INAA etc (Iwan Roelands 1987; Fassel 1978; Floyd et al, 1980).

#### **3.3.2 Preparation of standard solutions and instrument calibration**

Geochemical analysis is a comparison of an unknown rock sample, with a sample of known concentration having broadly similar characters for any particular element of interest. This requires a range of standards which should encompass the range expected in the unknowns.

The standards used in this study are four International Rock Standards (IRS) namely DNC-1, W-2, BHVO-1 and STM-1 and in-house standards 22-22, 22-7, 18-15 and 16-8 which were standardised with respect to the IRS. The international rock standards were mainly used for the calibration of the instrument while the in house standards were used mainly to check the drift of the instrument with time.

The instrument was recalibrated after every 4-5 analysis and the stability of the instrument was monitored by running one or more of in house standards as unknowns during any given group of analysis.

The standards were digested and brought into solution following same procedures as for unknown samples permitting automatic matching of the matrix. Blank solutions are also prepared by using the same reagents as for standards and unknown samples but without adding any powdered sample to it.

### 3.3.3 Precision and Accuracy

Precision is a measure of analytical repeatability. A precise analysis is one where a set of replicate analysis form a tight cluster about the average. The precision is governed by various factors such as weighing, instrumental precision, dilutions, sample homogeneity etc. Accuracy is a measure of how close the analysed data lie to the true data of the sample. The error will be the numerical difference between the two values. This depends on the standards used during chemical analysis. Since the standards used in this study were USGS standards which were analysed by various advanced analytical techniques, the accuracy of the data reported in this study is considered to be good. The following table shows the accuracy (Expressed as %) of major and trace Elements of IRS analysed by ICP-AES, with which the instrument was calibrated.



Table 3.2 Accuracy of major and trace element data of IRS (Analysed by ICP-AES) used for calibration of the instrument.

	REPORTED					OBTAINED					ACCURACY (%)				
	BHVO-1	W2-2	DNC-1	STM-1	RGM	BHVO	W2-2	DNC-1	STM-1	RGM	BHVO-1	W2-2	DNC-1	STM-1	RGM
Fe	11.120	4.84	8.94	-	-	11.085	4.66	9.07	-	-	0.32	3.69	1.5	-	-
Mg	7.20	3.18	10.05	-	-	7.11	3.08	10.14	-	-	1.22	3.00	0.89	-	-
Mn	0.17	0.08	0.15	-	-	0.167	0.081	0.152	-	-	1.22	0.66	1.34	-	-
Ca	11.40	5.44	-	-	-	11.467	5.29	-	-	-	0.59	2.71	-	-	-
Al	13.80	7.67	-	-	-	13.69	7.85	-	-	-	0.77	2.40	-	-	-
Ti	2.71	0.53	-	-	-	2.7116	0.54	-	-	-	0.06	1.58	-	-	-
Ba	-	182	-	560	-	-	171.95	-	562.9	-	-	5.5	-	0.53	-
Sr	-	194	-	700	-	-	184.42	-	702.4	-	-	4.9	-	0.35	-
Zr				1210	219				1210.7	212.39				0.058	3.0
	18 - 15	22 - 7				18 - 15	22 - 7				18 - 15	22 - 7			
Cr	3020.00	360.00				3026.70	370.31				0.04	2.06			
Ni	1048.00	320.00				1047.8	320.60				0.01	0.18			

W2-2 =, Twice the common dilution of IRS W-2 (only for Major elts).

## CHAPTER - 4

### Geochemical Results and Discussion

The Chemical data obtained on the major and trace elements of the mafic rocks of the Hutti schist belt are given in Table 4-1. The major element oxide data for ten out of the twelve samples analysed totals between 97 and 101 percent, and the remaining two samples GH-13 and GH-16 totals to 90 and 91 percent respectively. The low totals on these two samples could be due to the abundance of chlorite and carbonates. The  $\text{SiO}_2$  content of the Hutti amphibolites is about 48.5% on the average and only in two samples GH-3 and GH-14 it crosses 50 weight percent. The Alumina content is about 15 weight percent on the average and does not show much variation. The high alumina content of the amphibolites indicates that the amphiboles could be of pargasitic composition. The  $\text{TiO}_2$  content is also high, about 1 weight percent on the average, and this could be due to the presence of ilmenite in the samples (Refer to Table 4-3). High amount of opaques (about 4 to 5%) in thin sections also supports this. The data on the concentration of iron is reported as  $\text{FeO(T)}$  and for norm calculations, it is assumed that there is no ferric iron. The rocks have high iron content, about 13 weight percent on the average, and plots in the Fe-Tholeiites field in the Jenson's AFM diagram (Fig. 4.1). The high iron content of the amphibolites of the Hutti schist belt may be significant in terms of gold mineralization. In the absence of an iron formation in the Hutti area, these Fe-rich tholeiites must have been responsible for trapping the sulfide bearing ore fluid by precipitating sulfide minerals like pyrite, arsenopyrite etc and thereby precipitating gold from the auriferous sulfide complexes.

Table 4.1

	GH-3	GH-4	GH-5	GH-7	GH-8	GH-10
SiO <sub>2</sub>	55.8	49.08	48.22	49.70	48.9	48.40
TiO <sub>2</sub>	1.06	1.30	1.25	1.30	0.84	0.74
Al <sub>2</sub> O <sub>3</sub>	14.25	15.00	15.75	12.75	16.00	16.00
Feo (T)	14.33	13.03	13.35	13.23	11.73	10.78
MnO	0.23	0.19	0.20	0.18	0.20	0.18
MgO	4.15	6.63	7.45	9.33	7.40	9.33
CaO	6.98	12.18	11.90	10.43	14.00	12.5
Na <sub>2</sub> O	2.40	2.10	2.15	2.00	2.00	1.9
K <sub>2</sub> O	0.37	0.20	0.20	0.36	0.15	0.37
Total	99.57	99.71	100.47	99.28	101.22	100.20
Zr	72	82	80	71	44	41
Ni	89	118	154	275	181	211
Cr	29	166	257	690	221	310
Ba	104	22	43	64	33	56
Sr	142	178	182	221	146	102
Mg#	0.353	0.489	0.511	0.570	0.542	0.618
[Mg]	10.5	14.5	15.8	18.9	15.7	19.2
[Fe]	99.5	13.8	13.6	13.7	11.8	10.8
T°Ol	1121.3	1156.2	1180.0	1240.8	1166.5	1227.2
T°pl	1169.5	1180.5	1191.9	1136.1	1192.0	1186.9
EqFo	58.6	73.9	76.1	79.8	78.4	83.6
EqAn	74.6	78.3	79.3	73.9	80.6	80.8

(Table 4.1 contd..)

	GH-11	GH-12	GH-13	GH-14	GH-16	GH-17
SiO <sub>2</sub>	45.50	46.23	45.06	51.98	45.27	48.8
TiO <sub>2</sub>	1.33	1.22	1.01	0.78	0.73	0.73
Al <sub>2</sub> O <sub>3</sub>	15.50	15.00	14.50	15.75	13.50	11.5
Feo (T)	13.45	13.08	11.40	10.75	12.38	10.10
MnO	0.21	0.20	0.17	0.21	0.27	0.19
MgO	7.90	7.35	6.05	7.65	8.53	10.45
CaO	12.50	11.70	11.45	10.78	8.43	12.60
Na <sub>2</sub> O	1.95	1.80	1.30	1.40	0.95	1.70
K <sub>2</sub> O	0.25	0.28	0.27	0.39	0.12	0.94
Total	98.59	96.86	91.21	99.69	90.18	97.01
Zr	82	76	41	37	36	56
Ni	144	132	162	173	161	154
Cr	252	211	275	281	270	690
Ba	48	40	35	56	22	510
Sr	135	133	64	90	38	451
Mg#	0.523	0.512	0.498	0.571	0.561	0.661
[Mg]	16.6	15.9	14.2	16.5	18.1	21.8
[Fe]	13.3	13.7	13.1	12.0	14.2	10.3
T°Ol	1194.8	1182.4	1145.6	1181.7	1227.4	1272.5
T°pl	1176.9	1184.3	1186.2	1180.0	1165.8	1096.0
EqFo	77.6	76.2	74.3	79.1	78.4	86
EqAn	82.0	80.6	84.3	84.0	86.1	71.3

**Table 4.1 (a) : Symbols used in the text and tables.**

[Mg] - Compositionally corrected Mg

[Fe] - Compositionally corrected Fe

T<sup>°</sup>Ol - Olivine Saturation Surface temperature

T<sup>°</sup>Pl - Plagioclase Saturation Surface temperature

EqFo - Forsterite content of Olivine at T<sup>°</sup>Ol

EqAn - Anorthite Content of Plagioclase at T<sup>°</sup>Pl

Mg# - Mg/Mg+Fe all in Cation mole Fractions.

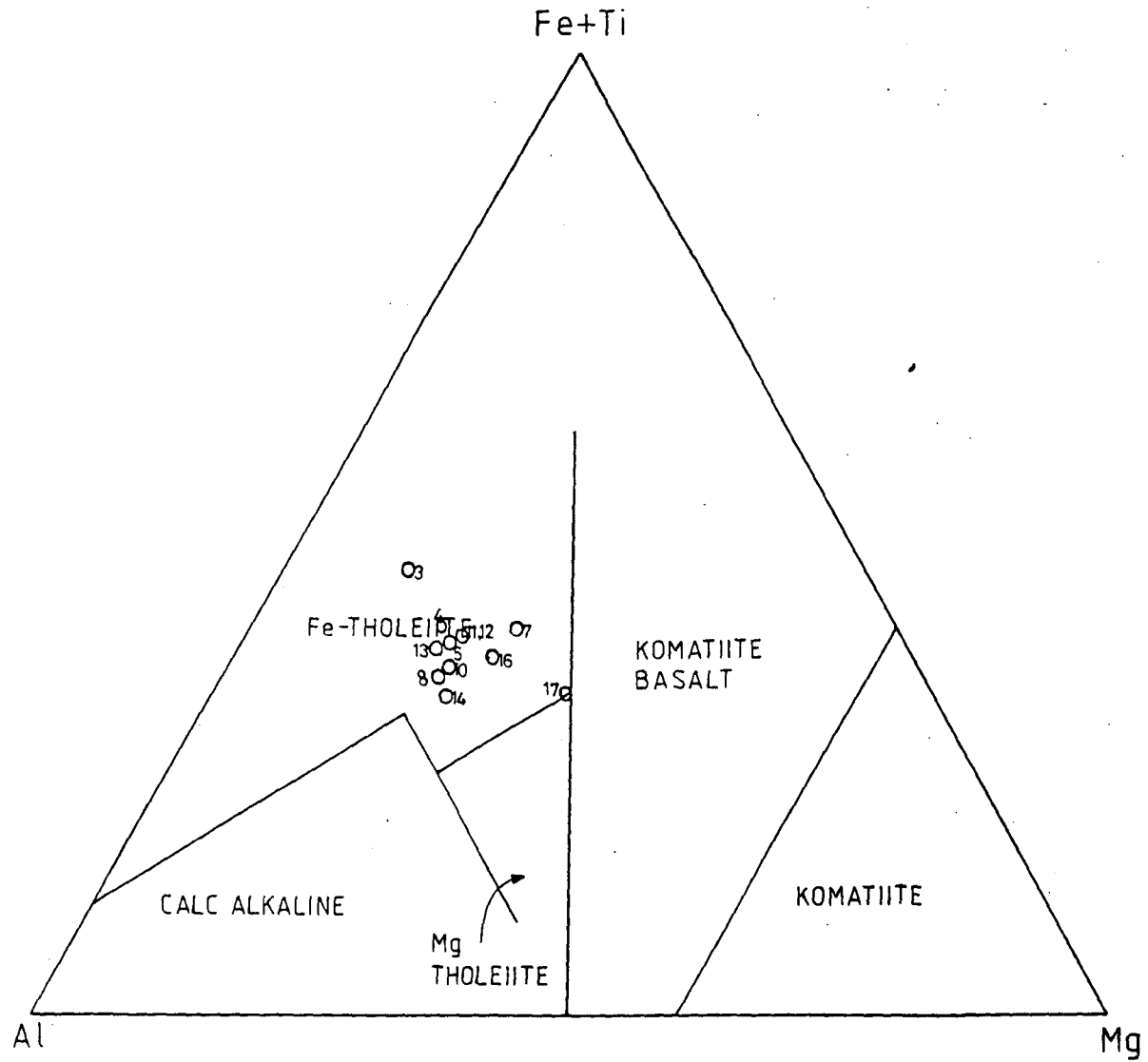


Fig. 4.1: Fe + Ti-Mg-Al ternary diagram (Jenson, 1976) for the classification of Huttu metabasalt.

**Table 4.2 Calculated Cation mole percentages of Hutti Meta tholeiites**

Sample No	GH-3	GH-4	GH-5	GH-7	GH-8	GH-10
SiO <sub>2</sub>	53.47	46.28	44.92	46.74	45.08	44.63
TiO <sub>2</sub>	0.76	0.92	0.88	0.92	0.58	0.51
Al <sub>2</sub> O <sub>3</sub>	16.09	16.67	17.29	14.13	17.38	17.39
FeO	11.48	10.27	10.40	10.40	9.04	8.31
MnO	0.19	0.15	0.16	0.14	0.16	0.14
MgO	5.93	9.32	10.35	13.08	10.17	12.83
CaO	7.17	12.30	11.88	10.51	13.83	12.35
Na <sub>2</sub> O	4.46	3.84	3.88	3.65	3.57	3.40
K <sub>2</sub> O	0.45	0.24	0.24	0.43	0.18	0.44

(Table 4.2 contd...)

Sample No	GH-11	GH-12	GH-13	GH-14	GH-16	GH-17
SiO <sub>2</sub>	43.14	44.76	46.58	48.82	47.13	46.44
TiO <sub>2</sub>	0.95	0.89	0.79	0.55	0.57	0.52
Al <sub>2</sub> O <sub>3</sub>	17.32	17.12	17.67	17.44	16.56	12.90
FeO	10.67	10.59	9.86	8.44	10.78	8.04
MnO	0.17	0.16	0.15	0.17	0.24	0.15
MgO	11.17	10.61	9.32	10.71	13.24	14.82
CaO	12.70	12.14	12.68	10.85	9.40	12.85
Na <sub>2</sub> O	3.58	3.38	2.61	2.55	1.92	3.14
K <sub>2</sub> O	0.30	0.35	0.36	0.47	0.16	1.14

The percentage of normative minerals in the Huttu meta tholeiites is given in Table 4-3. Out of the twelve samples analysed, two samples GH-3 and GH-14 are quartz normative, and sample GH-11 is nepheline normative. All other samples are neither quartz normative nor nepheline normative. The major element data presented in table 4-1 was converted into cation molecular proportions, since it will be easier to study the variations among samples in this form (Beswick, 1982). The recalculated cation mole percent of the major elements for the meta tholeiites of the Huttu belt are given in table 4-2. Out of the twelve samples analysed, six samples have  $T^{\circ}OI$  greater than that of  $T^{\circ}pl$  which means that olivine is the liquidus phase for these samples. For the remaining six samples, plagioclase is the liquidus phase. Two samples representing a primitive composition, based on their Mg numbers were selected for a rigorous major and trace element modelling.

#### **[Mg]-[Fe] Diagram**

Hanson and Langmuir (1978) and Langmuir and Hanson (1980) have used the Olivine saturation surface of Roeder and Emslie (1970) and calculated the melt and residue fields in a plot of MgO versus FeO in cation Mole percent, for batch melting of a pyrolite mantle using a FeO-MgO exchange reaction distribution coefficient ( $K_D$ ) between Olivine and basaltic melts of 0.3. The temperatures given in Fig 4-2 are for one atmosphere. A residue left behind after the removal of a melt from a pyrolite source would plot in the residue field and if the residue has only olivine, it would plot on the Olivine composition line marked in fig. 4.2.



**Table 4.3 Normative Mineral Composition (in percentage) of Mafic Rocks from Hutti Schist Belt. Fe<sub>2</sub>O<sub>3</sub> is assumed to be zero**

Sample No.	GH-3	GH-4	GH-5	GH-7	GH-8	GH-10
Quartz	9.14	0.00	0.00	0.00	0.00	0.00
Orthoclase	2.26	1.20	1.19	2.16	0.88	2.18
Albite	22.29	19.20	19.42	18.23	17.87	16.99
Anorthite	27.95	31.47	32.93	25.13	34.08	33.89
Nepheline	0.00	0.00	0.00	0.00	0.00	0.00
Diopside	6.30	24.05	21.17	21.93	28.05	22.29
Hypersthene	30.52	12.09	5.74	19.49	1.13	3.35
Olivine	0.00	10.16	17.81	11.22	16.82	20.28
Ilmenite	1.53	1.84	1.75	1.84	1.16	1.03

(Table 4.3 contd..)

Sample No.	GH-11	GH-12	GH-13	GH-14	GH-16	GH-17
Quartz	0.00	0.00	0.00	2.94	0.57	0.00
Orthoclase	1.51	1.73	1.78	2.34	0.80	5.71
Albite	14.29	16.90	13.03	12.75	9.59	15.68
Anorthite	33.59	33.48	36.76	36.05	36.22	21.55
Nepheline	2.19	0.00	0.00	0.00	0.00	0.00
Diopside	23.93	21.77	21.32	14.56	8.64	34.15
Hypersthene	0.00	7.18	22.90	30.27	43.05	3.74
Olivine	22.61	17.17	2.64	0.00	0.00	18.13
Ilmenite	1.90	1.78	1.57	1.10	1.14	1.04

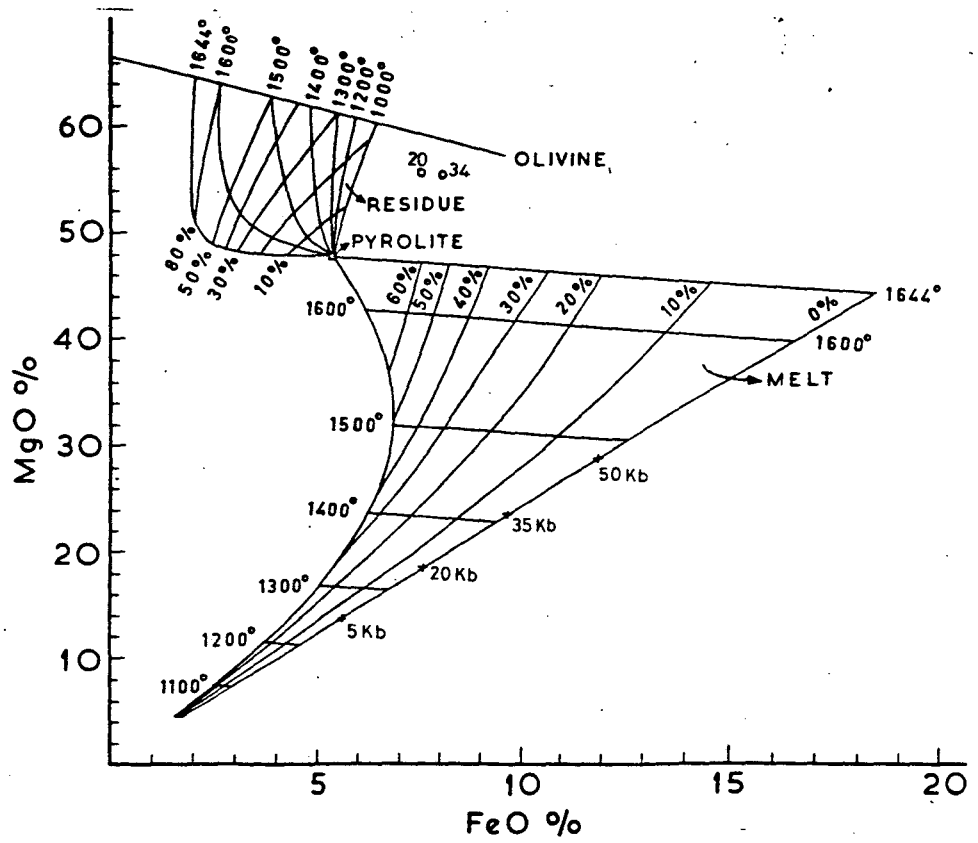


Fig. 4-2. Cation mole percent MgO Versus FeO diagram (Hanson and Langmuir, (1978). Symbols marked 5,20,35 and 50 kb are calculated solidil compositions for the respective pressures.

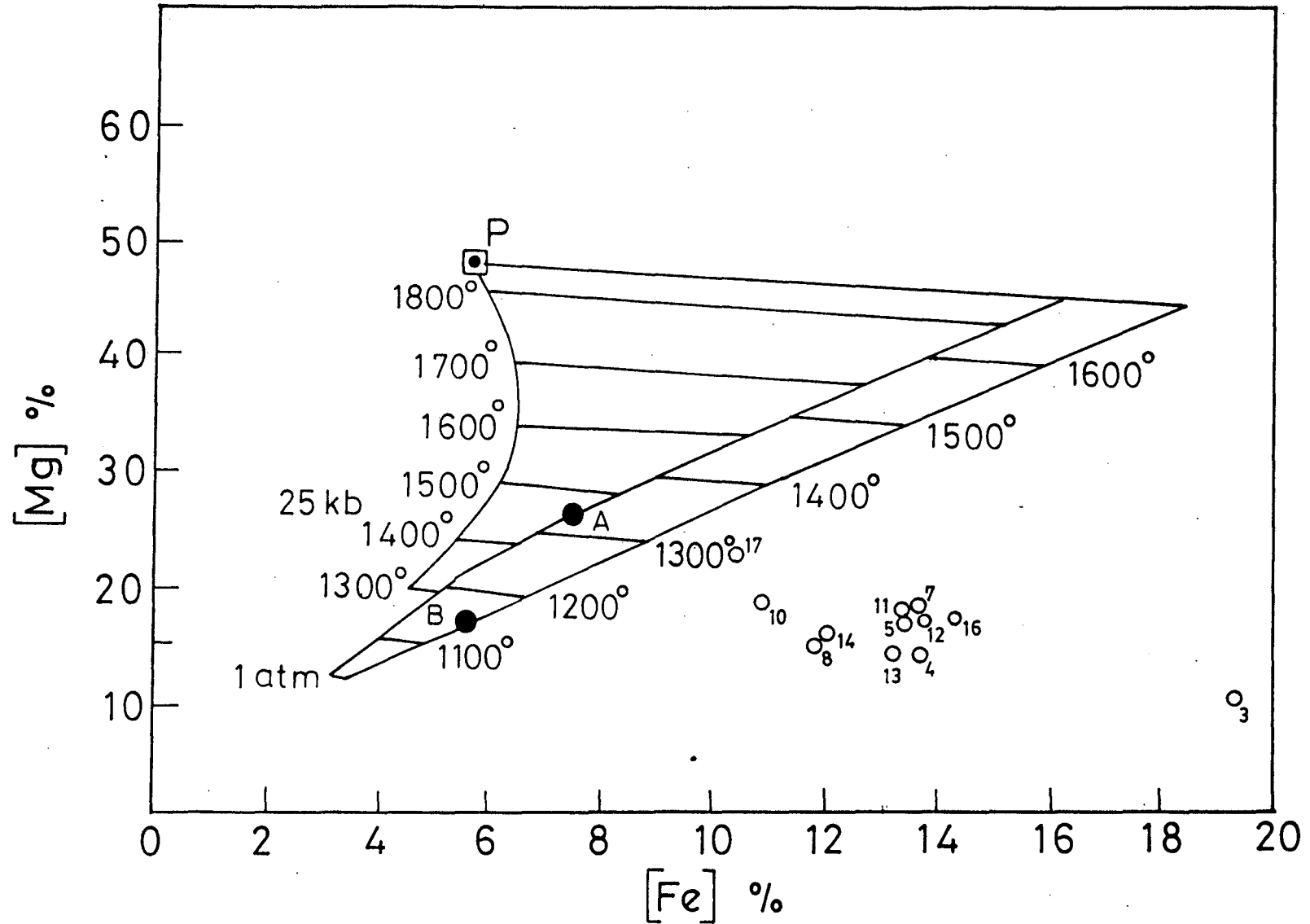


Fig. 4-3. [Mg] versus [Fe] diagram. A and B are calculated solidii for 25 kb and 1 atm pressure respectively. P denotes the assumed pyrolite source. Curve is a calculated melt evolution path on crystallisation of first olivine and then followed by pyroxenes.

Rajamani et al. (1985) subsequently modified the [Mg]-[Fe] diagram and included the pressure dependence of the melt. These authors calculated the melt fields for the melting of a pyrolite mantle (with 38.9 weight percent MgO and 7.6 wt. percent FeO) with isotherms at 25 Kbar and one atmosphere and extrapolated the same to 50 Kbar, considering an increase of 5°C per Kbar. These authors have discussed in detail the usefulness of the [Mg]-[Fe] diagram in assessing the magmatic differentiation processes and estimation of the pressure-temperature conditions of magma extraction.

The solidii for a pyrolite mantle source for 25 k bar and 1 atmosphere pressures are calculated and plotted in fig. 4.3. It is evident from fig 4.2, that as the extent of melting increases, the melt gets progressively depleted in "Fe". As the pressure of melting increases, the temperature of melt initiation increases and the melt formed becomes increasingly rich in Fe and Mg.

The compositionally corrected values of MgO and FeO designated as [Mg] and [Fe] for the Hutti meta tholeiites are calculated and plotted in Fig. 4.3, assuming that the parental liquids for these metavolcanics had equilibrated with Olivine, using relations derived by Ford et al (1983). .pn59

Except sample GH-3, all other samples are of basaltic composition and they plot in the Fe-tholeiite field of Jenson's AFM diagram. (Fig. 4.1). The Hutti meta tholeiites show a large spread on the [Fe], sub parallel to the [Fe]-axis, in the [Mg]-[Fe] diagram (Fig. 4.3). The position of datapoints in this diagram suggests that the magmas were derived under pressures of about 10-20 kb and temperatures between 1150°C and 1300°C. The parental magmas for the Hutti meta tholeiites could not have been derived from the assumed pyrolite source (Solidii A and B in fig. 4.3) since the position of data points would require atleast 50% fractional

Crystallization of Olivine followed by pyroxene and plagioclase, to be derivatives from such a melt. This much of fractionation would deplete the Ni content in the melt to about 30 ppm from 300 ppm. This would also affect the major elements drastically. But the Ni contents and the major element data obtained for the Hutti meta tholeiites do not support this.

Let us consider two samples GH-7 and GH-10 representing a primitive composition for [Mg]-[Fe] modelling. Both the samples have similar [Mg] values but there is a difference of 3 cation mole percent Fe between the two samples and hence a compositional gap along the [Fe]-axis in Fig. 4.3. If we assume that GH-7 is derived by fractional crystallization of GH-10, then it would require large extent of fractionation, which will drastically change the major element Chemistry and the composition of GH-7 will no longer be basaltic. The Ni and Cr contents of GH-7 should also be lower than GH-10. But this is not observed. So the possibility of fractional crystallization is ruled out. By incompatible element (Zr) modelling it can be checked whether these two samples were derived by different extents of melting which is indicated by the position of GH-10 and GH-7 in the [Mg]-[Fe] diagram.

If "D" for Zr is assumed as zero, then the batch melting equation becomes

$$\frac{C_1}{C_0} = \frac{1}{F} \Rightarrow F = \frac{C_0}{C_1}$$

If  $C_0$  is assumed as 10 ppm then the extent of melting will be

$$F = \frac{10}{41} = 0.24 = 24\% \text{ Melting [for (GH-10)]}$$

and  $F = \frac{10}{71} = 0.14 = 14\% \text{ Melting [for (GH-7)]}$

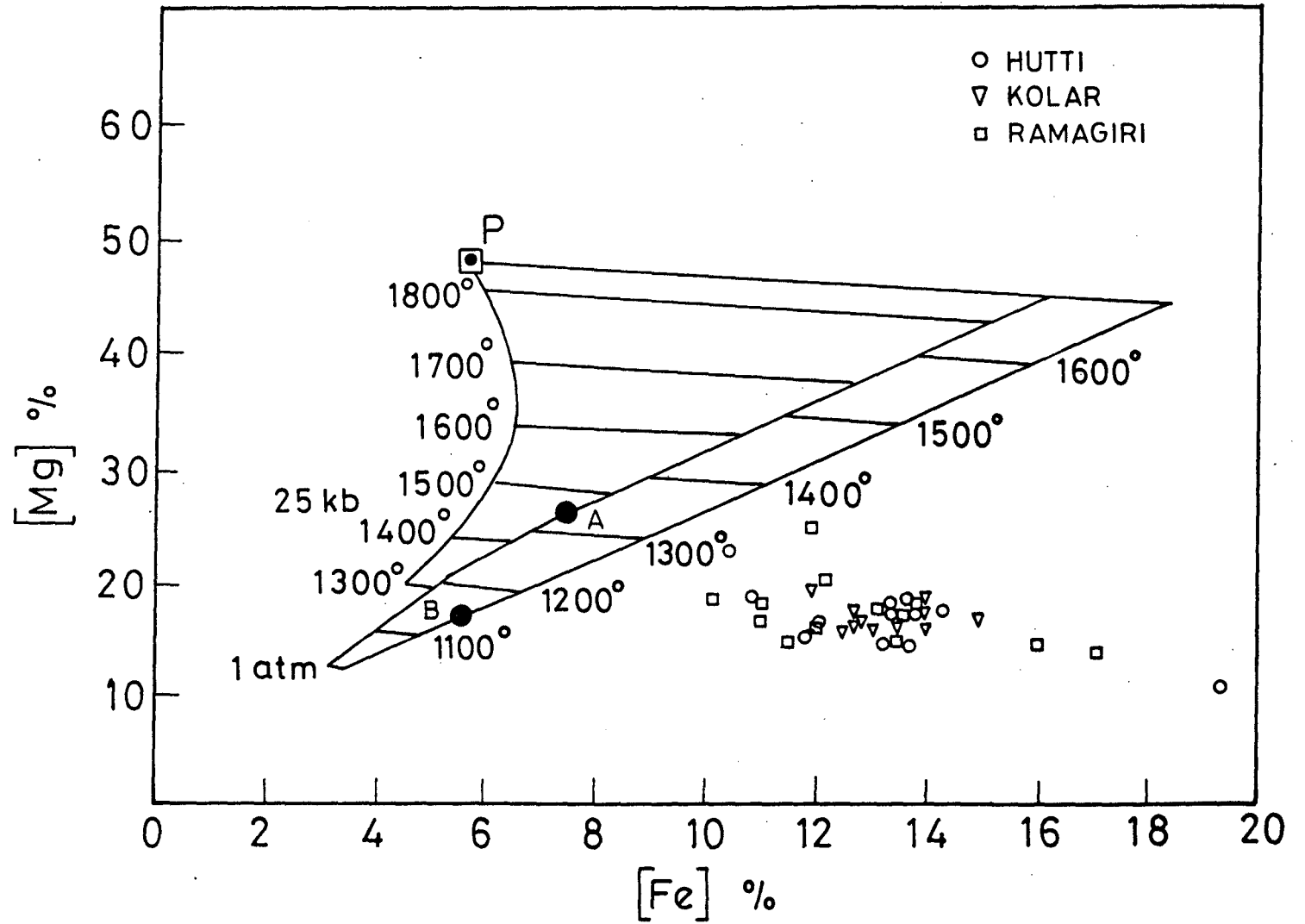


Fig. 4.4. Comparison of Hutti metatholeiites with the tholeiites of Kolar and Ramagiri in the [Mg] versus [Fe] plot.

Thus, we can arrive at a conclusion that the samples GH-10 and GH-7 were derived by higher and lower extents of melting respectively, of a source with lower MgO/FeO ratio than a pyrolite Mantle. The solidus for these two samples will have to plot to the right side of the sample point GH-7 in fig. 4-3. i.e., towards the higher [Fe] side, but with a similar [Mg] value.

Ni-Zr modelling of the Hutti metatholeiites (fig. 4-5) indicates that the rocks were formed by different extents of melting. In this modelling mantle source is assumed to have 2000 ppm Ni and 7.8 ppm Zr (Taylor and McLennan, 1981) and it consists of 55% Olivine, 25% orthopyroxene and 20% clinopyroxene. "D" for Ni is calculated for these three phases and the one atmosphere single element Olivine/melt distribution coefficients for Ni are 3 and 7.8 (Arndt, 1977b), for Opx-Melt are 1.5 and 3 and for Cpx-Melt are 1.0 and 2.7. (Irving, 1978) at 1600°C and 1450°C respectively. "Zr" is assumed to be incompatible and "D" for "Zr" is assumed as zero.

[Fe]-Zr modelling of the Hutti metatholeiites (fig 4.6), also indicates that the rocks were derived by different extents of melting. However this diagram also indicates some fractionation between samples GH-5, GH-4, GH-11 and GH-12. Having established that the samples GH-7 and GH-10 represents a somewhat primitive composition, we can determine whether the samples 4,5,11 and 12 were fractionated from this primitive composition, as indicated by the fig. 4.6.

Let us consider the sample GH-7 representing a primitive composition, and a sample GH-5 which is having a much lower abundance of Ni than GH-7. We can

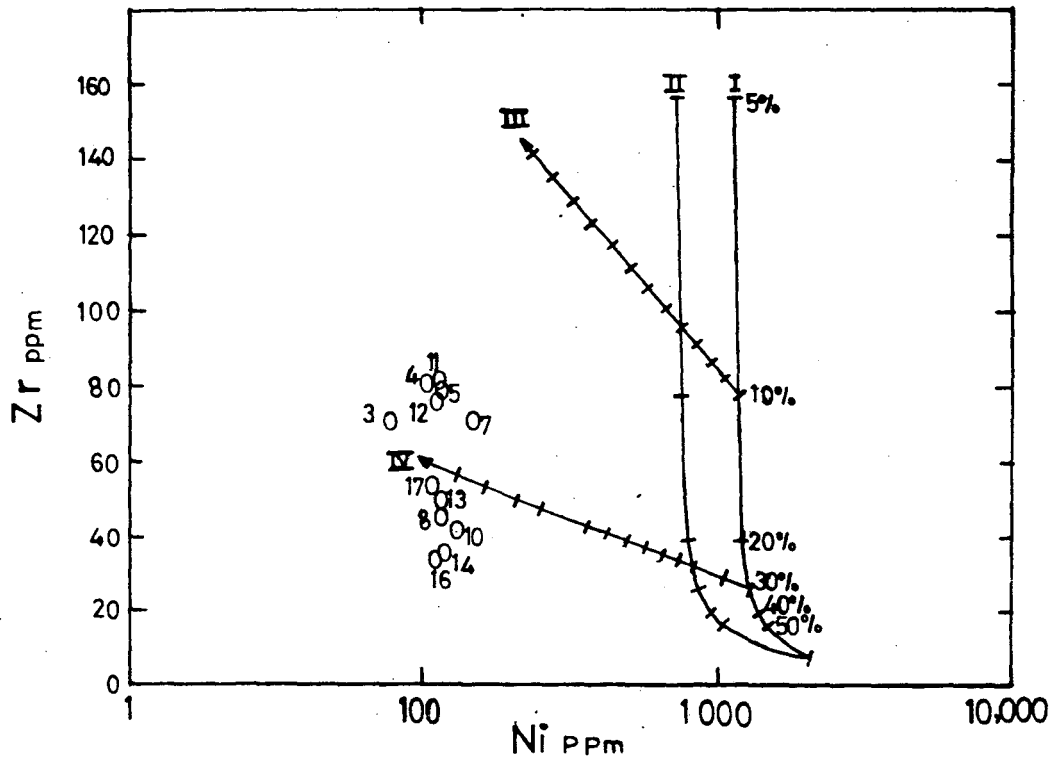


Fig. 4-5. Plot of Zr against Ni abundances in the Hutti amphibolites. Curves I and II are calculated batch melting curves at 1850°C, 50 kb and 1575°C, 25 kb respectively and are marked with percentages of melting. curves III and IV are olivine fractionation trends at one atmosphere with tics marking increments of 5% olivine fractionation from the previous tic.



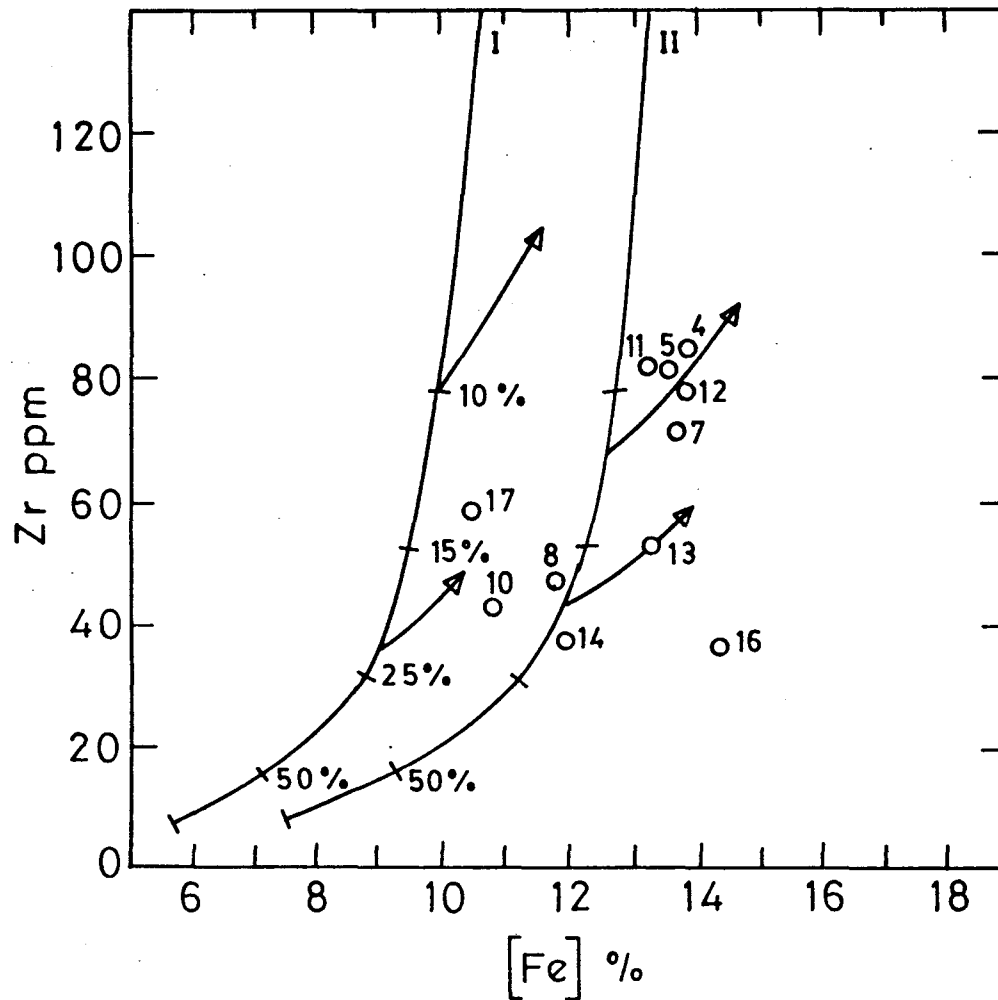


Fig. 4-6. Plot of Zr against [Fe] abundances in the Huttu metatholeiites. Curves I and II refer to batch melting curves calculated at 1850°C, 50 kb for mantles with 5.65 and 7.5 cation mole percent Fe, respectively. Zr is assumed to be incompatible. Curves with arrows are olivine fractionation trends at one atmosphere with a maximum of 25 percent fractionation.

determine whether GH-5 is a fractionated product of GH-7. It is also possible to determine the extent of olivine fractionation which gave rise to the present Ni content in sample GH-5, using equation 39 of Beattie et al. (1991), which is given as

$$D_i^{\alpha-L} = A_i^{\alpha-L} \cdot D_{Mg}^{\alpha-L} + B_i^{\alpha-L}$$

Where  $D_i^{\alpha-L}$  is the partition coefficient of the element between the phase in question and liquid, and  $A_i^{\alpha-L}$  and  $B_i^{\alpha-L}$  are empirical constants for the phase and the element  $i$ . The values of these constants are given in table-1 of the Beattie et al (1991). The phase " $\alpha$ " in which we are interested in is Olivine and the element " $i$ " of interest is "Ni". So the partition coefficient of Ni between Olivine and Liquid  $D_{Ni}^{OL-L}$  has to be determined using the above relation. A value of 10 was obtained for olivine- melt Kd for Ni. Using this Kd value and the equation for fractional crystallization,  $C_1/C_o - F^{D-1}$ , we calculate a 13% Olivine F.C from sample GH-7 to sample GH-5. A similar extent of Fractional Crystallization is calculated for an incompatible element such as Zr, between the two samples.

In the same way, a 12% Olivine fractional Crystallization has been calculated for samples GH-4, GH-11 and GH-12, from GH-7.

The Hutti Meta tholeiites were projected from the Diopside plane on to the plane of CA-M-S(Mole %) (O' Hara, 1968), and is shown in fig. 4-7. The plotting parameters for the CA-M-S projection are shown in the Table 4-4. The pressures obtained from this CA-M-S projection diagram is consistent with the one inferred from the [Mg]-[Fe] diagram. Among the two samples representing a primitive composition, GH-7 is formed at relatively higher pressures than sample GH- 10. This is also supported by the high Ni and Cr contents of the sample GH-7.

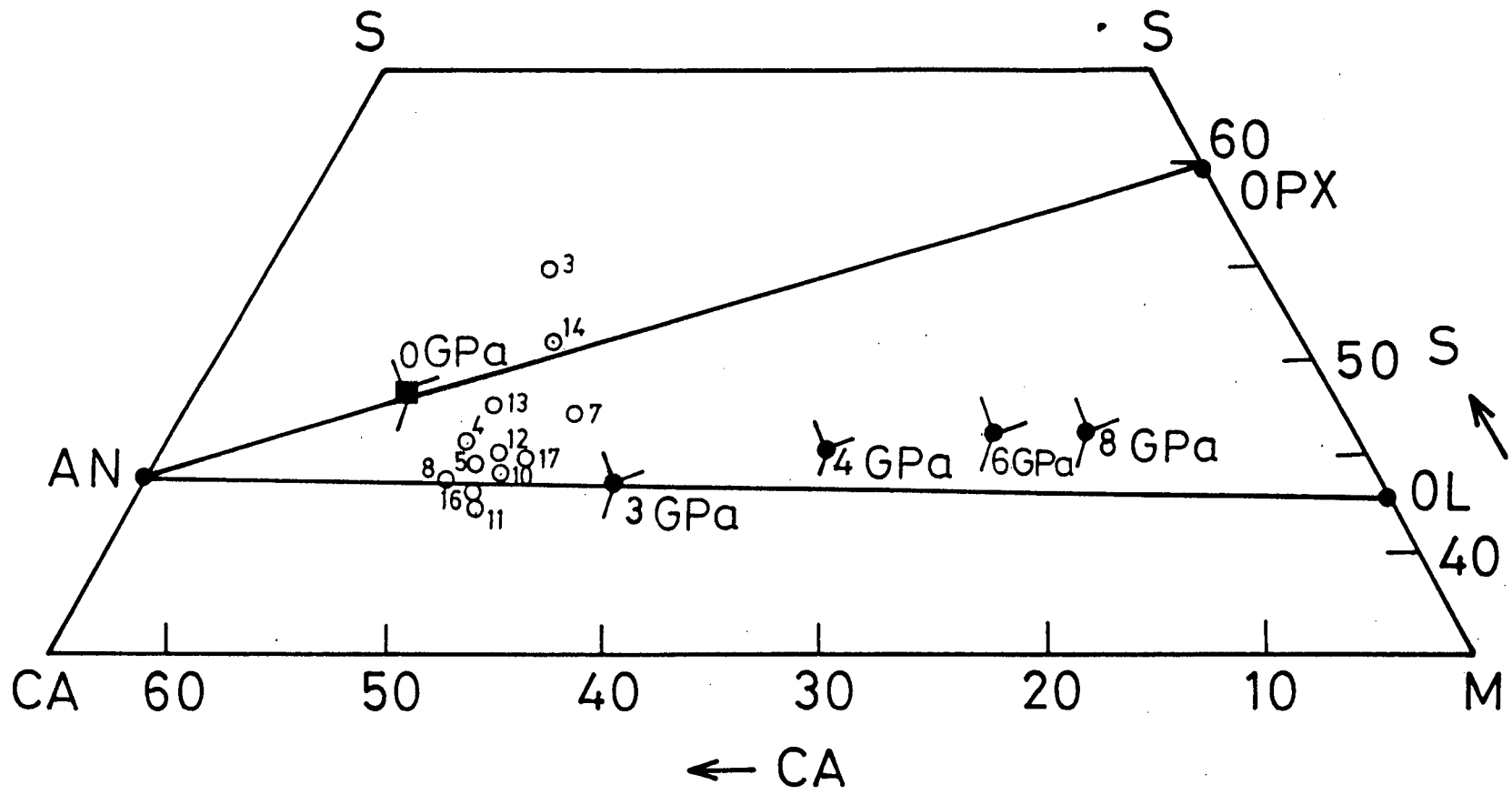


Fig. 4.7. CA-M-S projection diagram for the Hutti metatholeiites [After O'Hara (1968), modified by Herzberg et al (1990)] projected from the diopside plane on to the plane of CA-M-S (Mole Percent).

**Table 4-4****Plotting parameters for the CA-M-S projection Diagram for the Hutti Meta tholeiites.**

S.No.	Sample #	CA	M	S
1.	GH-3	33.93	12.31	53.75
2.	GH-4	41.87	12.99	35.14
3.	GH-5	41.78	14.37	43.85
4.	GH-7	36.58	16.89	46.53
5.	GH-8	44.36	12.55	43.08
6.	GH-10	41.50	14.96	43.54
7.	GH-11	43.20	15.29	41.51
8.	GH-12	41.10	14.77	44.13
9.	GH-13	39.92	12.85	47.23
10.	GH-14	36.11	13.41	50.49
11.	GH-16	31.45	17.92	50.63
12	GH-17	40.05	16.25	43.70

## CHAPTER - 5

### CONCLUSION

The Hutti meta tholeiites were compared with Kolar and Ramagiri Tholeiites in the [Mg]-[Fe] diagram. (Fig. 4.4) and there is a perfect overlapping of data points of all the three schist belts. The position of data points in the [Mg]- [Fe] diagram indicates that the source for the generation of Hutti metatholeiites cannot be a pyrolite mantle source as assumed, and the source should have a lower MgO/FeO ratio than a Pyrolite mantle. Such a source could be Komatiitic, generated by the melting of a Pyrolite mantle, at a pressure of about 30 Kbars and a temperature of about 1400°C. Melting of such a Komatiitic source can produce a tholeiite of composition obtained for the Hutti metabasalts. The physical conditions of magma generation appear to be similar for the tholeiites of all the three schist belts. The pressures of magma generation are about 10-20 Kbars and temperature ranges between 1150°C and 1300°C.

As to the processes of magma generation, it is evident from the geochemical modelling of major and trace elements that the Hutti metabasalts were formed by different extents of melting (10-30%) of similar sources and also by lower extents of fractional crystallization from a primitive composition (Sample # Gh-7) for some of the samples.

The Hutti metatholeiites bears geochemical similarities with that of Kolar metatholeiites in terms of magma type, in that both of them resemble magmas

generated at the midocean ridges. The homogeneity in rock assemblage, the uniformity of major element composition and the abundances of trace elements such as Zr, Ni, Cr and Ti for a suite of rocks, supports this idea and hence these two schist belts are different from the Ramagiri schist belt which has a heterogeneous rock assemblage and resemble magmas generated at the island arc setting. (Zachariah, 1992).

The Hutti schist belt differs from both Kolar and Ramagiri schist belts in terms of not possessing the Banded Iron Formation (BIF). The Hutti tholeiites also differs from Kolar and Ramagiri tholeiites in terms of having a slightly higher Fe content (13 wt% on the average).

The metabasalts of all the three schist belts have undergone brittle - ductile shearing and this must have provided the avenues for the fluids to pass through, resulting in the typical green schist facies alteration and mineralization. The nature of gold precipitating mechanism appears to be similar in all the three schists. The ore bearing fluids in the form of sulfide complexes must have reacted with the Fe - rich tholeiites, resulting in the precipitation of sulfide minerals like pyrite, arsenopyrite etc and gold must have been released and precipitated along with the silica. It has been reported by Phillips et al (1984) that the formation of pyrite from the sulfide complexes, leads to the effective reduction and precipitation of gold.

Detailed REE and isotopic studies have to be done to understand better the crustal evolution and mineralization in this part of the Dharwar craton.

## R E F E R E N C E S

- Abhinaba Roy (1979): Polyphase folding deformation in the Hutti-Maski schist belt, Karnataka. Jour. Geol. Soc. India, vol. 20, pp. 598-607.
- Abhinaba Roy and K.K. Raju (1980) : A note on the occurrence of olivine Dolerite dyke near Hutti, Raichur Dist, Karnataka. Jour. Geol. Soc. India, vol. 21, pp. 151-154.
- Anantha Iyer, G.V., and Vasudev, V.N., (1979): Geochemistry of the Archaean metavolcanic rocks of the Kolar and Hutti Gold fields. Jour. Geol. Soc. India, vol. 20, pp. 419-432.
- Anantha Iyer, G.V., Vasudev, V.N., and Jayaram. S., (1980) REE geochemistry of metabasalts from Kolar and Hutti gold bearing volcanic belts, Karnataka craton, India, Jour. Geol. Soc. India, vol. 21, pp. 603-604.
- Arndt, N.T., (1977) : Partitioning of Ni between olivine and ultrabasic and basic Komatiitic liquids. Yb. Carnegie. Instn. Wash., vol. 76, pp. 553-557.
- Balakrishnan. S., and Rajamani. V., (1987) : Geochemistry and Petrogenesis of granitoids around the Kolar schist belt, South India : Constraints for the evolution of the crust in the Kolar area, Jour. Geol., v-95, pp. 219-240.

Balakrishnan, s., Hanson, G.N., Rajamani, V., (1990) Pb and Nd isotope constraints on the origin of high Mg and tholeiitic amphibolites, Kolar schist belt, South India. Contrib. Mineral. Petrol, vol. 107, pp. 279-292.

Beswick, A.E., (1982) : Some geochemical aspects of alteration and genetic relations in Komatiitic suites. In KOMATIITES": N.T. Arndt, and E.G. Nisbet (eds), George Allen and Unwin.

Biswas, S.K., Prabhakaran, K., and Rao, P.S., (1985) : Preliminary exploration of auriferous lodes of Hutti-Maski Schist belt, Karnataka, India. U.N. Regional Seminar on gold exploration and development, Bangalore, sect. II; pp. 1-29.

Biswas, S.K., (1990) : Gold mineralization in the utiblock of Hutti-Maski supracrustal belt, Karnataka. Jour. Geol. Soc. India, vol. 36, pp. 79-89.

Chadwick, B., Ramakrishnan, M., Vasudev, V.N., and Viswanatha, M.N., (1989) : Facies distribution and structure of a Dharwar volcanosedimentary basin : Evidence for late Archaean transpression in southern India. Jour. Geol. Soc. London, vol. 146, pp. 825-834.

Claude Herzberg, (1992) : Depth and degree of melting of Komatiites. Jour. Geophys. Res. vol. 97, No. B4, pp. 4521- 4540.



Curtis, L.c., Radhakrishna, B.P., and Naidu, G.K., (1990) Hutti-Gold mine with a Future". Geol. Soc. Ind. Publication. 123 pages.

Drury, S.A., (1983) : The petrogenesis of setting of Archaean metavolcanics from Karnataka state, South India. Geochim. Cosmochim. Acta, vol. 37, p. 317-329.

Drury, S.A., Harris, N.B.W., Holt, R.W. Reeves Smith, G.J., and Wightman. R.T., (1984): Precambrian Tectonics and Crustal evolution in south India : Jour. Geol, Vol. 92, pp. 3-20.

Fassel, V.A., (1978): Quantitative elemental analysis by plasma emission spectroscopy, SCIENCE, v. 202, pp. 183-191.

Floyd, M.A., Fassel, V.A., and D'silva A.P. (1980) : Computer controlled scanning monochromator for the determination of 50 elements in geochemical and environmental sampies by ICP-AES. Anal. Chem., V. 52, pp. 2168-2172.

Hanson, G.N., and Langmuir, C.H., (1978): Modelling of Major elements in mantle melt systems using trace element approaches. Geochim. Cosmochim. Acta, v. 42, pp. 725-741.

Hanson, G.N., (1980): Rare earth elements in petrogenetic studies of igneous rocks. Annual. Rev. Earth. Planet. Sci., V.8, pp. 371-406.

Hanson, G.N., (1989): An approach to trace element Modelling using a simple igneous system as an example. In "Geochemistry and Mineralogy of Rare Earth Elements." B.R. LIPIN and G.A.Mckay (eds). Min. Soc. America.

Herzberg, C., Gasparik, T., and sawamoto. H., (1990). Origin of mantle peridotite : constraints from melting experiments to 16.5 Gpa, Jour. Geophys. Res. vol. 95, pp. 15, 799-15,803.

Jenson, L.S., (1976): A new method of classifying Subalkaline volcanic Rocks. Ontario division of Mines, Misc. Paper No. 66, p. 22.

Krogstad, E.J., Balakrishnan, S., Mukhopadhyay, D.K., Rajamani, V., and Hanson, G.N., (1989): Plate tectonics 2.5 billion years ago: Evidence at Kolar, South India. A report SCIENCE, v. 243, pp. 1337-1340.

Langmuir, C.H., and Hanson, G.N., (1980): An evaluation of major element heterogeneity in the mantle sources of basalts. Phil. Trans. R.Soc. London, v. A297, pp. 383-407.

Mahanty, S.C., and Raju, K.K., (1974) : Geology and methods of working at Hutti Gold Mines. Geol. Min. Met. Soc. India, v. 46, pp. 257-265.

Naqvi, S.M., (1981) : The oldest supra crustals of the Dharwar craton : Jour. Geol. Soc. India, v. 22, pp. 511-525.

Naqvi, S.M. and Rogers, J.J.W., (1983) : Introduction, in precambrian of South India. Memoir. Geol. Soc. India, v. 4, pp. 6-16.

O'Hara, M.J., (1968): The bearing of phase equilibria studies in synthetic and Natural systems on the origin and evolution of basic and ultrabasic rocks. Earth. Sci. Rev., v. 4, pp. 69-133.

Paul Beattie, Clifford Ford, and Douglas Russel (1991) : Partition Coefficients for Olivine - Melt and Orthopyroxene- Melt system. Contrib. Mineral. Petrol. v. 109, pp. 212-224.

Phillips. G.N., Groves. D.I., and Martyn, J.E., (1984); An epigenetic origin for Archaean Banded iron formation hosted gold deposits. Econ. Geol., v. 79, pp. 162-171.

Pichamuthu, C.S., and Srinivasan (1984) : A billion year history of the Dharwar craton. (3200 - 2100 m.y. ago). Memoir. Geol. Soc. India, v. 4, pp. 121-142.

Radhakrishna, B.P., (1983): Archaean granite-greenstone terrain of the South Indian shield, Memoir. Geol. Soc. India, v. 4, pp. 1-46.

Radhakrishna, B.P., and Naqvi, S.M., (1986) : Precambrian continental crust of India, and its evolution. Jour. Geol., v. 94, pp. 145-166.

Rajamani, v., Shivkumar, K., Hanson, G.N., and Shirey, S.B., (1985): Geochemistry and petrogenesis of Amphibolites, Kolar schist belt, South India : Evidence for Komatiitic magma derived by Low percentages of melting of the mantle. Jour. Petrol., v. 26, Part - 1, pp. 92-123.

Rajamani, V., Shirey. S.B., and Hanson. G.N., (1989) Fe-rich Archaean tholeiites derived from Melt-enriched mantle sources : Evidence from the Kolar schist belt, South India. Jour. Geol. v. 97, pp. 487-501.

Rajamani, V., (1990) : Petrogenesis of Metabasites from the schist belts of the Dharwar craton : Implications to Archaean Mafic Magmatism. Jour. Geol. Soc. India. v. 36, pp. 565-587.

Rajamani, v., (1991) : "Gold Mineralization in the transect corridor." Geol. Soc. India - Workshop on "Deep continental crust of India," pp. 115-117.

Ramakrishnan. M., Viswanatha, M.N., and Swaminath, J., (1976): Basement-Cover relationship of peninsular gneisses with highgrade schists and greenstone belts of southern karnataka. Jour. Geol. Soc. India, v. 17, pp. 97-111.

Roelandts, I., (1988) : Comparison of inductively coupled plasma and Neutron Activation Analysis for precise and accurate determination of nine rare earth elements in geological materials. Chem. Geol, v. 67; pp. 171-180.

Safonov, Yu. G., Radhakrishna, B.P., Krishna Rao, B., Vasudev, V.N., Krishna Raju. K., Nosik, L.P. and Pashkov. Y.N., (1980) : Mineralogical and geochemical features of epigene gold and copper deposits of South Inida. Jour. Geol. Soc. India, v. 21, pp. 365-378.

Sivasiddaiah. N., and Rajamani, V., (1989) : The geological setting, mineralogy, geochemistry and genesis of gold deposits of the Archaean Kolar schist belt, India. Econ. Geol. v. 84, pp. 2155-2172.

Sivasiddaiah. N., Hanson, G.N., and Rajamani. V., (in Preparation) : Rare earth element evidence for the syngenetic origin of an Archaean stratiform gold sulfide deposit, Kolar schist belt, South India.

Shapiro. L., and Brannock. W.W., (1962) : Rapid Chemical analysis of silicate, carbonate and Phosphate rocks. U.S. Geol. Surv. Bull. v. 1144 A, pp. 56.

Swaminath, J., and Ramakrishnan. M., (1981) : Early Precambrian supracrustals of Southern Karnataka, Memoirs. Geol. Surv. India, v. 112, pp. 79-87.

Taylor, S.R., and Mc Lennan, S.M., (1981) : The Composition and evolution of the continental crust : Rare Earth Element evidence from Sedimentary rocks. Phil. Trans. R. Soc. London., vol. A-301, pp. 381-399.

Vasudev. V.N., and Naganna. C :, (1973) : Mineragraphy of gold quartz - Sulfide reefs of Huttigold Mines, Raichur Dist, Mysore state. Jour. Geol. Soc. India, v. 14, pp. 378-383.

Zachariah (1992) : Geochemistry and petrogenesis of amphibolites of Ramagiri gold fields, south India. Unpublished Ph.D. thesis, Jawaharlal Nehru University, New Delhi.

Ziauddin, M., and Narayanaswamy. S., (1974): Gold Resources of India. Bull. Geol. Surv. India, v. 38., pp. 114-116.

Plate - 1

**Fig. 2.5:** The amphibolites of the madriankota area in tectonic contact with the granite. Pen is oriented E-W which is the trend of the Foliation.

**Fig. 2.6 :** Xenoliths of metabasalts in the Leucocratic granite indicating the intrusive nature of the contact in the Uti area.





Plate - 2

**Fig. 2.7 :** F3 type open folds in the amphibolites in the chinchargi area. Pen marks the axial plane of the fold which is oriented N15°E.

**Fig. 2.8 :** Pyroclastics associated with chlorite schist in the Pamankallur area.



Plate - 3

**Fig. 2.9 :** Underformed clastic pebbles embedded in a darker finegrained matrix in the conglomerate horizon of the Palkanmardi area. The pebbles are of granitic composition.

**Fig. 2.10 :** Stretched granitic pebbles in the conglomerates of the Palkanmardi area. The pebbles are stretched parallel to the foliation of the matrix and the pebbles themselves have a gnessic foliation.

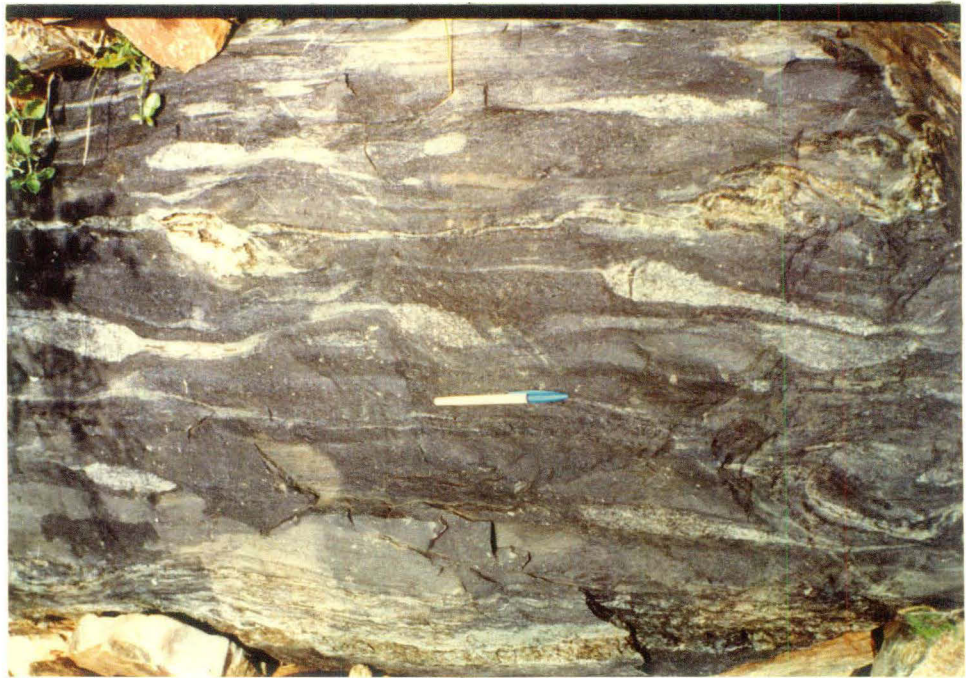


Plate - 4

**Fig. 2.11 :** Hornblende "augen" in a coarse grained amphibolite with plagioclase matrix swerving around the "augen". The augen could have formed as a result of shearing in two different directions, one cutting the other at a lower angle. Under crossed Nicols, Magnification-25x.

**Fig. 2.12 :** Actinolite grain is deformed and granulated giving rise to patchy extinction in a single grain, in sample GH-4. Under crossed nicols, magnification- 25x.

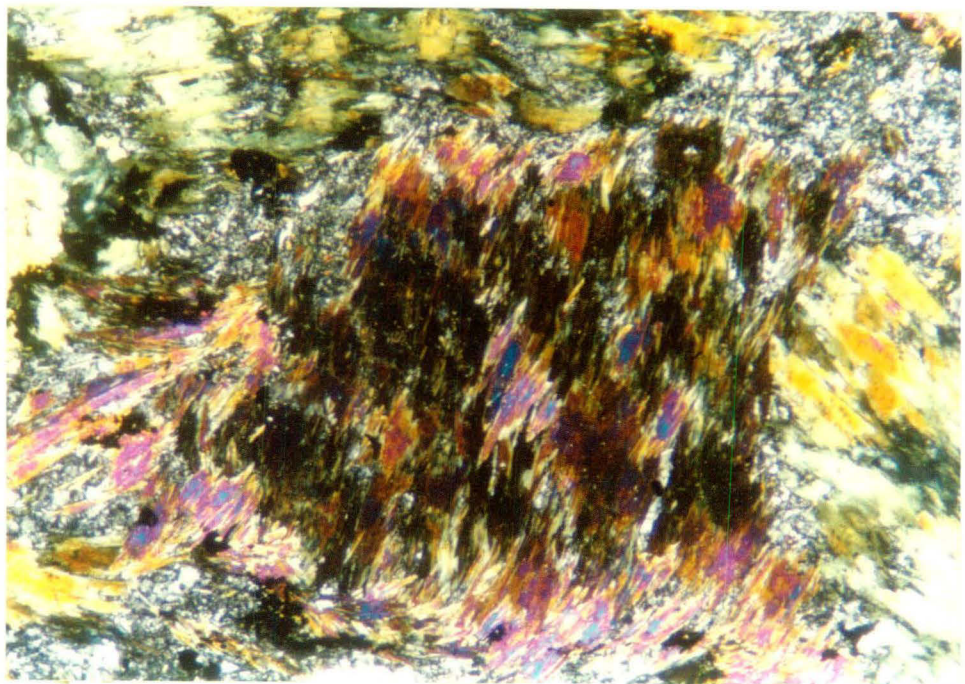
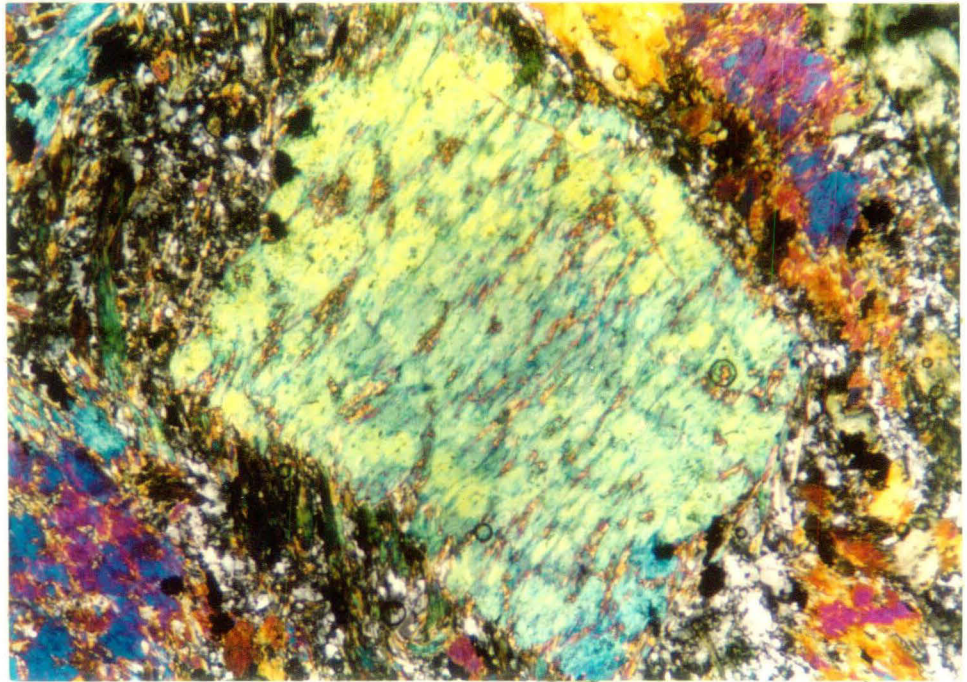


Plate - 5

**Fig. 2.13 :** Schistose amphibolite (sample # GH-7) east of Palkanmardi area showing two generations of hornblende (i) Prismatic hornblende and (ii) Euhedral (idioblastic) hornblende-formed probably due to reheating by the nearby granitic intrusion, since it is close to the contact. Under crossed Nicols. Magnification - 25x.

**Fig. 2.14 :** Fibrous aggregates of actinolite in sample GH-14, near pamankallur. Under crossed nicols, magnification - 25x.

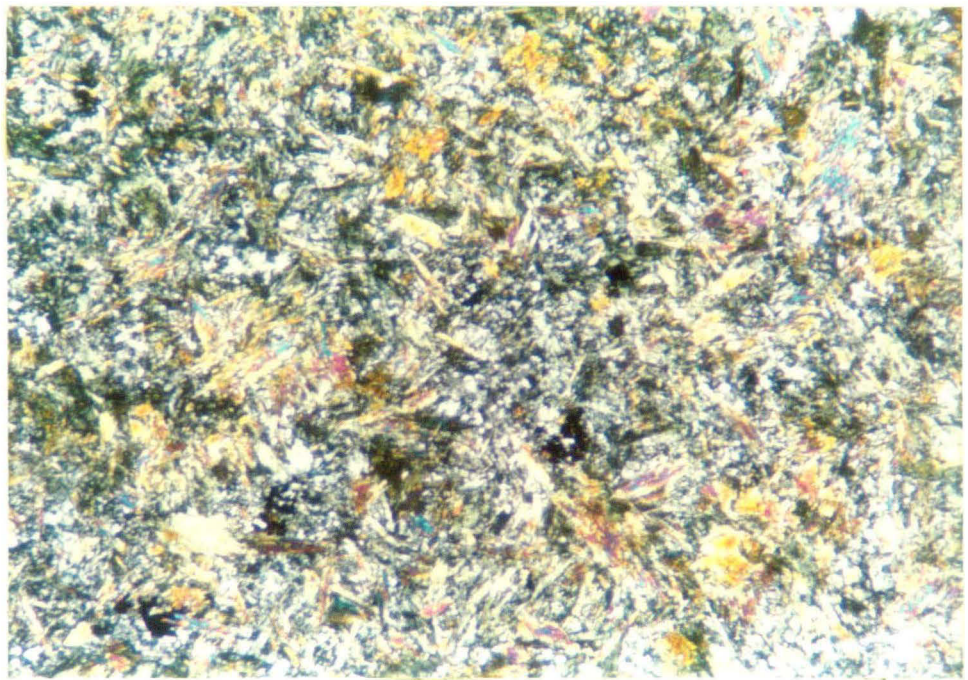
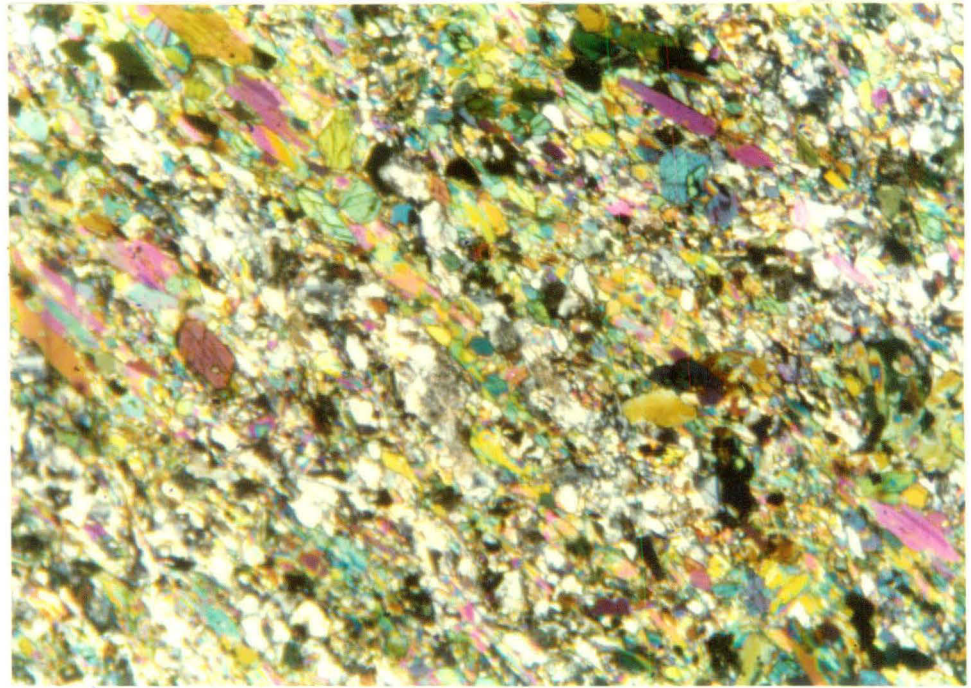




Plate - 6

**Fig. 2.15 :** Trident shaped calcite vein in the chlorite schist from pamankallur area. (sample # Gh-13). The calcite vein gives the appearance of a schist belt and the chlorite matrix gives the appearance of the granitoids surrounding the schist belt-for the simple reason that the schist belts have taken the strain and are more deformed than the granitoids. Under crossed Nicols, Magnification - 25x.

**Fig. 2.16 :** Calcite vein cutting the schistosity in the chlorite schist. (sample GH-13). Under crossed Nicols, Magnification - 25x.

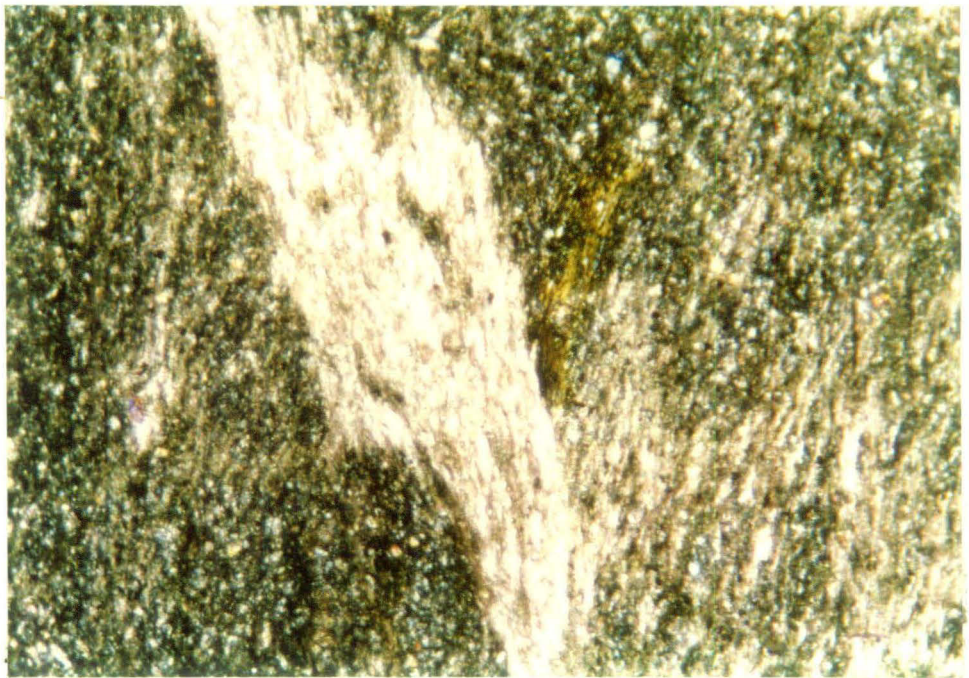
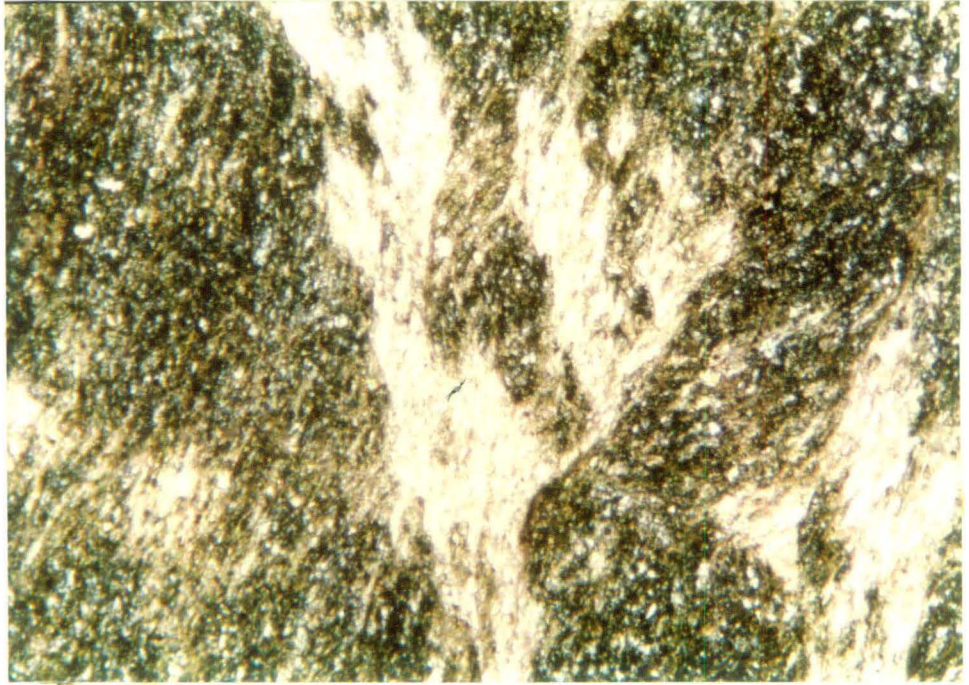


Plate - 7

**Fig. 2.17 :** Higher amount of opaques in the amphibolite. (sample # GH-4). The opaques could be ilmenite as indicated by the normative mineral composition. (Table 4.3). Under parallel Nicols, Magnification - 25x.

**Fig. 2.18 :** One big crystal of clinopyroxene (at the centre) altering to actinolite (Blue int. colour) and Epidote (Bright green int. colour) in sample # GH - 17, near the western contact. Under crossed Nicols, Magnification - 25x.

